The Arctic Surface Climate in CMIP6: Status and Developments since CMIP5

RICHARD DAVY AND STEPHEN OUTTEN

Nansen Environmental and Remote Sensing Center, and Bjerknes Center for Climate Research, Bergen, Norway

(Manuscript received 28 December 2019, in final form 27 May 2020)

ABSTRACT

Here we evaluate the sea ice, surface air temperature, and sea level pressure from 34 of the models used in phase 6 of the Coupled Model Intercomparison Project (CMIP6) for their biases, trends, and variability, and compare them to the CMIP5 ensemble and ERA5 for the period 1979 to 2004. The principal purpose of this assessment is to provide an overview of the ability of the CMIP6 ensemble to represent the Arctic climate, and to see how this has changed since the last phase of CMIP. Overall, we find a distinct improvement in the representation of the sea ice volume and extent, the latter mostly linked to improvements in the seasonal cycle in the Barents Sea. However, numerous model biases have persisted into CMIP6 including too-cold conditions in the winter (4-K cold bias) and a negative trend in the day-to-day variability over ice in winter. We find that under the low-emission scenario, SSP126, the Arctic climate is projected to stabilize by 2060 with an annual mean sea ice extent of around 2.5 million km^2 and an annual mean temperature 4.7 K warmer than the early-twentieth-century average, compared to 1.7 K of warming globally.

1. Introduction

The Arctic is of special importance in Earth's climate system as it is especially sensitive to changes in global forcing, such as the enhanced forcing from the build-up of greenhouse gases (GHGs). This is exemplified by Arctic amplification: during the latter half of the twentieth century the Arctic has warmed at around twice the rate of the global average temperature, and this is most pronounced in the winter (Johannessen et al. 2004). There are numerous factors behind this Arctic amplification. While much attention has been given to the sea ice albedo feedback (Serreze et al. 2009; Kumar et al. 2010), the recent Arctic amplification is driven by a reduction in the outgoing longwave radiation (OLR) and the reduction in the albedo, which primarily affects the absorption of shortwave radiation (Lesins et al. 2012; Dai et al. 2019). There are numerous processes that affect the OLR such as the Planck feedback (Planck 1901), the lapse-rate feedback (Manabe and Wetherald 1975), the water vapor feedback (Graversen and Wang 2009), changes in the atmospheric (Overland and Wang 2010) and oceanic (Spielhagen et al. 2011) heat transport, and changes to the cloud cover (Vavrus 2004). These changes to the surface energy budget lead to strong temperature changes in the Arctic due to the persistent stable stratification found in this region (Davy and Esau 2016). This signal of Arctic amplification is robust and has also been identified in paleoclimate records (Dahl-Jensen et al. 1998; Masson-Delmotte et al. 2006; Brigham-Grette et al. 2013). Global climate models need to be able to capture this important feature of climate change so they must include a reliable representation of the relevant processes. A recent review of the relative importance of these processes in contributing to Arctic amplification within global climate model results from phase 5 of the Coupled Model Intercomparison Project (CMIP5) indicated that it is local temperature feedbacks that are largely responsible for the recent Arctic amplification (Pithan and Mauritsen 2014). This is the process whereby the warmed air is trapped near the surface by the persistent stable stratification found in the Arctic, which leads to a greater warming in the Arctic than elsewhere (Esau et al. 2012).

Understanding the Arctic climate processes, and being able to simulate them within a global climate model,

Denotes content that is immediately available upon publication as open access.

Supplemental information related to this paper is available at the Journals Online website: https://doi.org/10.1175/JCLI-D-19-0990.s1.

Corresponding author: Richard Davy, richard.davy@nersc.no

DOI: 10.1175/JCLI-D-19-0990.1

is essential if we are to understand the future climate in the Arctic as we go toward a new climatology of a "blue Arctic" (i.e., summers free of sea ice). This is a dramatic shift in the Arctic climatology and will bring profound changes to the natural environment in the region (Descamps et al. 2017), as well as the potential for human activities in the region, such as through increased potential to use Arctic shipping routes (Smith and Stephenson 2013; Melia et al. 2016). As such there has been a lot of focus on when the Arctic will become (nearly) free of sea ice in the summers (Overland and Wang 2013). Attempts to estimate when this will happen involve either extrapolating from the observational record of sea ice volume (Maslowski et al. 2012) or analyzing global climate model projections (Pavlova et al. 2011; Wang and Overland 2012; Screen 2018; Notz and Stroeve 2018; Sigmond et al. 2018). The projected rate of sea ice loss in the twenty-first century depends upon the amount of sea ice in the historical period (Massonnet et al. 2012), but since this was not prescribed, there are large differences between the models in terms of sea ice extent, volume, and variability. Of these, sea ice volume provides the most comprehensive measure of the evolution of Arctic sea ice since it decreases faster than sea ice area (Kwok et al. 2009; Stroeve et al. 2012), although sea ice thickness is the primary cause for uncertainty in sea ice evolution between the models (Boé et al. 2010). The uncertainty in estimating when we can expect ice-free summers can be constrained by subsampling the CMIP5 model ensembles based on their climatology and evolution of sea ice during the end of the historical period (Massonnet et al. 2012).

Many small-scale processes have been identified as important in determining the Arctic climatology. These processes can be hard to represent accurately in global climate models due to either the relatively coarse resolution of these models or a limited understanding of these processes and their interactions. As such, the parameterization of small-scale processes can introduce biases into the Arctic climatology in these models. For example, Davy and Esau (2016) demonstrated the importance of shallow boundary layers in enhancing climate forcing signals. This can be very important in the Arctic, which frequently has shallow, stably stratified boundary layers. However, global climate models have systematic biases toward overestimating boundary layer mixing under stable stratification (Seidel et al. 2012; Davy 2018), which has been shown to lead to significant underestimation of the surface air temperature response to forcing (Davy and Esau 2014). There are also systematic biases introduced due to the representation of mixed-phase clouds (Pithan et al. 2014; Tan et al. 2016), sea ice albedo (Karlsson and Svensson 2013; Koenigk et al. 2014), sea ice extent (Stroeve et al. 2012), sea ice variability, and timing of the melting and freezing over the annual cycle (Mortin et al. 2014).

There are many variables that are important in shaping the Arctic climate related to the climatology and tendency of the atmosphere and sea ice. So, in the interest of brevity, here we limit ourselves to looking at sea ice through the lens of extent, thickness, and volume and at the atmospheric dynamics and thermodynamics using the surface air temperature and sea level pressure because these capture the fundamental aspects of the atmospheric thermodynamics and dynamics and help us relate this analysis to previous studies (Chapman and Walsh 2007).

In section 2 we present the data and methods used in the paper; in section 3 we review the state of the Arctic climate in CMIP5 and CMIP6, and compare this to that in ERA5; in section 4 we present the projections for the twenty-first century under different forcing scenarios prescribed in CMIP6; and in section 5 we present our conclusions about the skill of CMIP6 models in capturing the current Arctic climate, the uncertainty in projections for the twenty-first century, and how this picture has changed since the CMIP5 generation.

2. Data and methods

Here we use data from the CMIP5 and CMIP6 that have been made publicly available through the Earth System Grid Foundation web portal (https://esgf-data.dkrz.de/). For the CMIP5 simulations we use data from the historical and representative concentration pathway (RCP) scenarios. And for the CMIP6 simulations we use data from the historical and shared socioeconomic pathways (SSP) scenarios. For each of these scenarios we acquired the sea ice concentration and volume data at monthly resolution, the sea level pressure data at 6-hourly resolution, and the surface air temperature at daily resolution. The total Arctic sea ice extent and volume were calculated by multiplying the grid cell area by the sea ice concentration and thickness fields respectively, and then taking the sum of these for the whole Northern Hemisphere. For the other variables we applied a filter for the Arctic that selected only those data north of 66°N. The full lists of CMIP5 and CMIP6 models used are presented in Tables 1 and 2, along with the availability of the variables we have used in the different scenarios. There are quite large differences in the number of models for which a given variable is available for a given scenario. For example, there are many CMIP6 models that have surface air temperature and sea ice concentration data available, but not subdiurnal sea level pressure or monthly sea ice volume.

We compare the CMIP model results to the fifth generation European Centre for Medium-Range Weather Forecasts (ECMWF) reanalysis (ERA5) for the surface air temperature, sea level pressure, and sea ice extent;

TABLE 1. List of CMIP5 models used in the analysis presented here, which variables were available for each scenario in the analysis presented here, and the model resolution. SAT is surface air temperature, PSL is sea level pressure, SIE is sea ice extent, and SIV is sea ice volume.

CMIP5 model name	Variables available: historical	Variables available: RCP 8.5	Horizontal resolution
ACCESS 1.0	SAT, PSL, SIE, SIV	SAT, PSL, SIE, SIV	192 × 145
ACCESS 1.3	SAT, PSL, SIE, SIV	SAT, PSL, SIE, SIV	192 × 145
BCC-CSM1	SAT, PSL, SIE, SIV	SAT, PSL, SIE, SIV	128 × 64
BCC-CSM1M	SAT, PSL, SIE, SIV	SAT, PSL, SIE, SIV	320 × 160
BNU-ESM	SAT SIE, SIV	SAT SIE, SIV	128 × 64
CanCM4	SAT SIE, SIV	SAT	128 × 64
CanESM2	SAT, PSL, SIE, SIV	SAT, PSL, SIE, SIV	128 × 64
CCSM4	SAT, SIV	SAT	288 × 192
CESM1-BGC	SAT, SIV	SAT	288 × 192
CESM1-CAM5	SAT, SIV	SAT	288 × 192
CESM1-FASTCHEM	SAT, SIV	SAT	288 × 192
CMCC-CESM	SAT SIE, SIV	SAT SIE, SIV	96 × 48
CMCC-CM	SAT SIE, SIV	SAT, PSL, SIE, SIV	480 × 240
CMCC-CMS	SAT SIE, SIV	SAT SIE, SIV	192 × 96
CNRM-CM5	SAT SIE, SIV	SAT, PSL, SIE, SIV	256 × 128
CNRM-CM5–2	SIV	—	256 × 128
CSIRO-Mk3.6.0	SAT SIE, SIV	SAT SIE, SIV	192 × 96
CSIRO-Mk3L12	SIE, SIV	—	64 × 56
EC-EARTH	SAT, PSL, SIE, SIV	PSL, SIE, SIV	320 × 160
FGOALS-g2	SAT, PSL, SIE, SIV	SAT, PSL, SIE, SIV	128 × 60
FGOALS-s2	PSL, SIE, SIV	PSL, SIE, SIV	128 × 108
FIO-ESM	SAT, SIE, SIV	SAT, SIE, SIV	128 × 64
GFDL-CM2.1	SIE, SIV	—	144 × 90
GFDL-CM3	SAT, PSL, SIE, SIV	SAT, PSL, SIE, SIV	144 × 90
GFDL-ESM2G	SAT, PSL, SIE, SIV	SAT, PSL, SIE, SIV	144 × 90
GFDL-ESM2M	SAT, PSL, SIE, SIV	SAT, PSL, SIE, SIV	144 × 90
GISS-E2-H	SAT, PSL, SIE, SIV	SAT, PSL, SIE, SIV	144 × 90
GISS-E2-H-CC	SAT, SIE, SIV	SAT, SIE, SIV	144 × 90
GISS-E2-R	SAT, PSL, SIE, SIV	SAT, PSL, SIE, SIV	144 × 90
GISS-E2-R-CC	SAT, SIE, SIV	SAT, SIE, SIV	144 × 90
HadCM3	SAT, SIE, SIV	SAT	96 × 73
HadGEM2-AO	SIE, SIV	SIE, SIV	192 × 145
HadGEM2-CC	SAT, PSL, SIE, SIV	SAT, PSL, SIE, SIV	192 × 145
HadGEM2-ES	SAT, PSL, SIE, SIV	SAT, PSL, SIE, SIV	192 × 145
INM-CM4	SAT, PSL, SIE, SIV	SAT, PSL, SIE, SIV	180 × 120
IPSL-CM5A-LR	SAT, PSL, SIE, SIV	SAT, PSL, SIE, SIV	96 × 96
IPSL-CM5A-MR	SAT, PSL, SIE, SIV	SAT, PSL, SIE, SIV	144 × 143
IPSL-CM5B-LR	SAT, PSL, SIE, SIV	SAT, PSL, SIE, SIV	96 × 96
MIROC-ESM	SAT, PSL, SIE, SIV	SAT, PSL, SIE, SIV	128 × 64
MIROC-ESM-CHEM	SAT, PSL, SIE, SIV	SAT, PSL, SIE, SIV	128 × 64
MIROC4h	SAT, PSL, SIE, SIV	SAT,	640 × 320
MIROC5	SAT, PSL, SIE, SIV	SAT, PSL, SIE, SIV	256 × 128
MPI-ESM-LR	SAT, PSL, SIE, SIV	SAT, PSL, SIE, SIV	192 × 96
MPI-ESM-MR	SAT, PSL, SIE, SIV	SAT, PSL, SIE, SIV	192 × 96
MPI-ESM-P	SAT, PSL, SIE, SIV	SAT	192 × 96
MRI-CGCM3	SAT, PSL, SIE, SIV	SAT, PSL, SIE, SIV	320 × 160
MRI-ESM1	SAT, PSL, SIE, SIV	SAT, PSL, SIE, SIV	320 × 160
NorESM1-M	SAT, PSL, SIE, SIV	SAT, PSL, SIE	144 × 96
NorESM1-ME	SAT, SIV	SAT	144 × 96

and we compare the sea ice volume from the climate models to that from the Pan-Arctic Ice Ocean Modeling and Assimilation System (PIOMAS) reanalysis (Zhang and Rothrock 2003; Schweiger et al. 2011). Both of these products are reanalyses and so while they are constrained by observations, they still suffer from biases due to the underlying model; see Schweiger et al. (2011) for an evaluation of PIOMAS and Wang et al. (2019), Graham et al. (2019), and Frederiksen (2018) for evaluations of ERA5 in the Arctic. ERA5 does use observations of the

TABLE 2. List of CMIP6 models used in the analysis presented here, which variables were available for each scenario used in the analysis presented here, and the model resolution. SAT is surface air temperature, PSL is sea level pressure, SIE is sea ice extent, and SIV is sea ice volume.

CMIP6 model name	Variables available: historical	Variables available: SSP 126	Variables available: SSP 585	Horizontal resolution
AWI-CM1–1-MR	SAT, SIV	SAT, SIV	SAT	384 × 192
BCC-CSM2-MR	SAT, PSL, SIE, SIV	SAT, SIV	SAT, SIV	320 × 160
BCC-ESM1	SAT, SIE, SIV	—	—	128 × 64
CAMS-CSM1–0	SAT, SIE, SIV	SAT, SIE, SIV	SAT, SIE, SIV	320 × 160
CanESM5	SAT, SIE	SAT, SIE	SAT, SIE	128 × 64
CESM2	SAT, SIE, SIV	SAT, SIE, SIV	SAT, SIE, SIV	288 × 192
CESM2-WACCM	SAT, SIE, SIV	SAT, SIE, SIV	SAT, SIE, SIV	288 × 192
CNRM-CM6–1	SAT, PSL, SIE, SIV	SAT, SIE, SIV	SAT, SIE, SIV	256 × 128
CNRM-CM6–1-HR	SAT, SIE, SIV	—	—	720 × 360
CNRM-ESM2–1	SAT, PSL, SIE, SIV	SAT,	SAT,	256 × 128
E3SM-1–0	SAT, SIE	—	—	360 × 180
EC-Earth3	SAT, PSL, SIE, SIV	SAT, SIE	SAT, SIE	512 × 256
EC-Earth3-Veg	SAT, PSL, SIE, SIV	SAT, SIE	SAT, SIE	512 × 256
FGOALS-f3-L	SAT	SAT	SAT	288 × 180
FGOALS-g3	SAT, PSL	SAT	SAT	180 × 80
GFDL-CM4	SAT, PSL, SIE, SIV	—	SAT, SIE, SIV	288 × 180
GFDL-ESM4	SAT, SIE, SIV	SAT, SIE, SIV	SAT, SIE, SIV	288 × 180
GISS-E2–1-G	SAT, PSL, SIV	—	—	144 × 90
GISS-E2–1-G-CC	SAT, SIV	—	—	144 × 90
GISS-E2–1-H	SAT, SIE, SIV	—	—	144 × 90
HadGEM3-GC31-LL	SAT, SIE, SIV	—	—	192 × 144
INMCM-4.8	SAT, SIE	SAT, SIE	SAT, SIE	180 × 120
INMCM-5.0	SAT, SIE	—	—	180 × 120
IPSL-CM6A-LR	SAT, PSL, SIE, SIV	SAT, SIE, SIV	SAT, SIE, SIV	144 × 143
MCM-UA-1–0	SAT, SIE	SAT	SAT	96 × 80
MIROC6	SAT, SIE	SAT, SIE	SAT, SIE	256 × 128
MIROC-ES2L	SAT, SIE	SAT, SIE	SAT, SIE	128 × 64
MPI-ESM1–2-HR	SAT, PSL, SIE, SIV	SAT, SIE, SIV	SAT, SIE, SIV	384 × 192
MRI-ESM2–0	SAT, PSL, SIE	SAT, SIE	SAT, SIE	320 × 160
NESM3	SAT, PSL, SIE	SAT, SIE	SAT, SIE	192 × 60
NorCPM1	SAT, SIE	—	—	144 × 96
NorESM2-LM	SAT, SIE, SIV	—	—	144 × 96
SAM0-UNICON	SAT, PSL, SIE, SIV	—	—	288 × 192
UKESM1–0-LL	SAT, SIE, SIV	SAT, SIE, SIV	SAT, SIE, SIV	192 × 144

sea ice extent from HadISST and satellite-derived products (http://www.osi-saf.org), which have well-constrained uncertainties, but ERA5 has been shown to suffer from warm biases under extremely cold conditions (Wang et al. 2019) which is likely related to the representation of strongly stable atmospheric boundary layers (Steeneveld 2014).

We chose to compare the climatology from the models and the reanalysis over the period 1979–2004 because this covers the period of satellite observations (from 1979) when the reanalysis is well constrained by observations and finishes at the end of the historical scenario protocol of the CMIP5 in 2004. We therefore argue that choosing this period provides the fairest comparison between the CMIP5 and CMIP6 model results. The time series were computed using the native grid of each model, and the maps of the ensemble means were calculated by first regridding each model output onto a standard grid of 0.5° × 0.5° using bilinear interpolation and then computing ensemble means. Some models had more than one simulation of a given scenario (i.e., multiple ensemble members). To include all of these in the climatologies we first took an ensemble mean for the individual model across these different simulations so that each model only had one contribution to the multimodel ensemble. However, for the calculation of autoregression and variability we calculated these for each simulation individually and then averaged over all simulations for a given model to get the average properties of that model.

Note that in CMIP5 we only have the variable *sit*, which is the volume-per-unit-area of sea ice in a given grid cell. In CMIP6 this variable is now called *sivol*. In PIOMAS this same information is referred to as the effective sea ice thickness. It is these three variables, which have the same meaning, that we use throughout this paper when we are analyzing the sea ice volume or sea ice thickness.

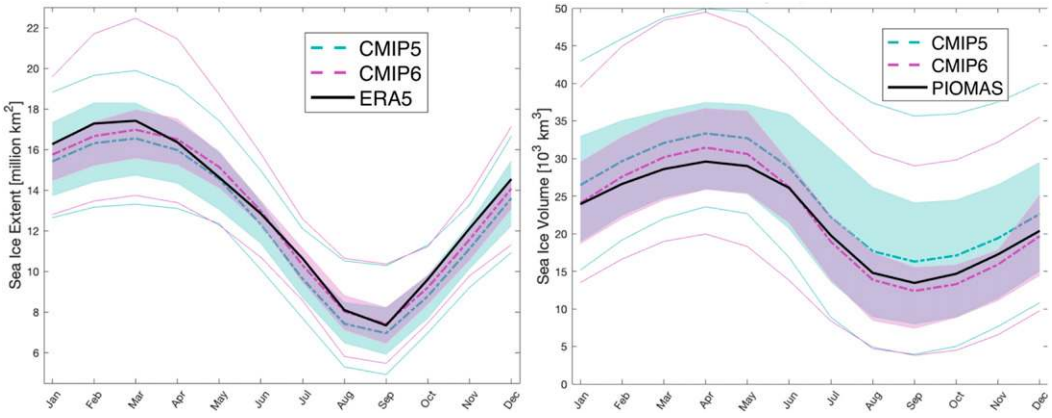

FIG. 1. The climatology of the Arctic sea ice (left) extent and (right) volume for the period 1979–2004. The CMIP5 models are shown in turquoise and the CMIP6 models are in purple. The shaded areas show the range between the 25th and 75th percentiles of the model ensembles; the thick dashed lines show the ensemble mean; and the thin lines show the 5th and 95th percentiles of the ensemble. The thick black line shows the climatology from the ERA5 for the extent and from PIOMAS for the volume.

For each monthly time series we converted the data to anomalies by removing the full-period climatological mean for each month. For the daily surface air temperature data, we took an area-weighted mean over the Arctic, and then calculated the standard deviation within each month to create a monthly time series describing the day-to-day variability in the Arctic. We also took the standard deviation within each month of the daily-mean temperature for each grid point to create a monthly time series for each location. This process was repeated for the 6-hourly sea level pressure data to create a time series of the intramonthly variability in the Arctic-mean sea level pressure and a monthly time series for each grid cell of the intramonthly variability in sea level pressure. We then converted each of these variables into anomalies by removing the climatological average for each month, calculated from the full period.

The intra-annual autoregression was calculated by taking a linear regression of the anomaly in a given month against the anomaly from the previous month. For example, the intra-annual autoregression of temperature in March was calculated by taking the linear regression of the March temperature anomalies against the February temperature anomalies. This process was repeated for all variables for which we calculated the intramonthly autoregression.

3. Representation of the present climate

a. Sea ice

1) CLIMATOLOGY

Sea ice cover is crucial in determining the climatology of the Arctic region. This is because sea ice acts to decouple the exchange of heat, moisture, momentum, aerosols, and other tracers between the ocean and atmosphere. Therefore, differences in the sea ice concentration and extent can lead to large differences in the surface energy budget, and consequentially the Arctic climatology. Sea ice thickness has been noted as one of the largest sources of uncertainty in the evolution of sea ice (Zygmuntowska et al. 2014). There is an inverse relationship between sea ice thickness in the Arctic Ocean and sea ice export, both in the interannual variability and in the long-term trends, that has been demonstrated to hold for a selection of CMIP5 models (Langehaug et al. 2013). Biases in sea ice thickness may also be expected to affect the surface air temperature since thicker sea ice is associated with colder surface air temperatures (Labe et al. 2018). While this relationship is expected to be found within any given model, it does not necessarily hold for intermodel comparisons because parameters associated with the sea ice and atmospheric models may have been tuned independently, leading to different surface air temperature climatologies given the same sea ice thickness and underlying ocean state.

Figure 1 shows the climatology of the total Arctic sea ice extent and volume in CMIP5, CMIP6, and ERA5 for the period 1979–2004. The sea ice extent in ERA5 varies from around 17.4 million km^2 at the peak extent in March to a minimum of around 7.3 million km^2 in September. Both the CMIP5 and CMIP6 model ensembles capture the seasonal cycle with a close agreement between the multimodel means and the ERA5 climatology—the ERA5 sea ice extent lies within the 25th–75th percentiles of both ensembles at all times. Overall the CMIP6 ensemble mean has a closer

agreement to the ERA5 than does the CMIP5 mean (root-mean-square error of 0.59 million km^2 for CMIP6 compared to 0.92 million km^2 for CMIP5) and has a better fit at both the seasonal minima in September and the maxima in March. However, both the CMIP5 and CMIP6 means are biased toward underestimating the sea ice extent with a bias of −0.71 million km^2 in CMIP5 and −0.22 million km^2 in CMIP6. The bias does change with season but it is almost always smaller in CMIP6 than in CMIP5; for example, in March it is −0.46 and −0.89 million km^2 and in September it is +0.08 and −0.38 million km^2 for CMIP6 and CMIP5 respectively. While this indicates a clear improvement in CMIP6, individual models in both the CMIP5 and CMIP6 ensembles can have very large biases in the sea ice extent of up to 7 million km^2 and there is a wider ensemble spread in the March extent for CMIP6 than there is for CMIP5.

The climatology of the sea ice volume presents a different picture. In PIOMAS the Arctic sea ice volume changes from a peak of almost 30 000 km^3 in April, to a minimum of around 13 400 km^3 in September. The CMIP5 multimodel mean has a clear positive bias in all months with an average of 2900 km^3, whereas the CMIP6 mean has a negligible bias of 80 km^3, although the CMIP6 ensemble does have a larger annual cycle than does PIOMAS. Note that this bias in the CMIP5 ensemble mean lies outside of the PIOMAS uncertainties, which range from 1350 to 2800 km^3 in September and March respectively (Schweiger et al. 2011). Corresponding to this improvement in the bias, there is a reduction in the root-mean-square error in the sea ice volume from CMIP5 to CMIP6 of 2900 to 1200 km^3. While many of the models in CMIP6 seem to do a much better job of capturing the annual cycle, as seen in the reduced spread between the 25th and 75th percentiles of the two ensembles, there are still some models in the CMIP6 ensemble that have very large errors compared to PIOMAS, as characterized by the 95th percentile of the distributions (Fig. 1).

Figure 2 shows the sea ice thickness for the CMIP5 and CMIP6 ensemble mean, and the difference between the two ensembles, for the months of March and September and for the annual mean. The climatological mean of the effective sea ice thickness has a remarkable geographical consistency between the CMIP5 and CMIP6 ensembles in all months and in the annual mean. In the annual mean the CMIP6 ensemble mean has much thicker (up to 1 m) sea ice in the Canadian archipelago and somewhat thicker (~30 cm) ice in Fram Strait compared to the CMIP5 ensemble. Both observational and high-resolution sea ice models indicate that the thickest sea ice should be found around the Canadian archipelago (Kwok 2018). While CMIP6 models tend to have thick ice in this region, individual models vary greatly in the location of the thickest ice; for example, in NorESM2-LM the thickest ice (8 m thick) is found off the coast of northeast Greenland whereas in CESM2 the thickest ice is similarly about 8 m but is found in the northwest of the Canadian archipelago, so we find a large intermodel spread in the sea ice thickness across this region (Fig. S1 in the online supplemental material). The pattern of thicker ice in CMIP6 over the Canadian archipelago can be found in all months. The Canadian archipelago is a particularly challenging region for sea ice modeling in climate models because of the highly broken land cover and the challenges of capturing sea ice interactions with the land in such complex terrain (Kwok 2015). The simulated climatology of sea ice in this region is therefore sensitive to both the horizontal resolution of the model and the sea ice physics. There is also thick ice in many of the Canadian lakes in the CMIP6 ensemble, which was not present in CMIP5.

At the seasonal maximum in March we see that the CMIP6 ensemble has thinner ice over most of the Arctic, which is reflected in the lower overall sea ice volume seen in Fig. 1. The biggest difference in the September climatology is in the northernmost Canadian archipelago: in CMIP6 the models have relatively thick ice here (>2 m), whereas in CMIP5 the ice in this region was relatively thin or not present. In the CMIP6 ensemble the ice in September is also generally thicker (20–50 cm) across most of the Arctic basin. In the annual mean these seasonal differences in the Arctic basin largely cancel out, and the difference between the CMIP5 and CMIP6 ensembles is small compared to the mean thickness (<10 cm across most of the Arctic).

Figure 3 shows the bias in the sea ice thickness for the CMIP5 and CMIP6 ensemble means with respect to the PIOMAS simulations for the months of March and September and the annual mean. The sea ice extent from the ensemble means and ERA5 are also highlighted with thick red and black lines, respectively.

First, we can see that in almost all locations and times both the CMIP5 and CMIP6 ensemble means have slightly thinner sea ice than is found in PIOMAS. A clear exception is in the Canadian archipelago where the models have much thicker ice than PIOMAS, up to 2 m more, but also in those locations where the models simply have a larger extent than is found in PIOMAS. The bias in sea ice extent is shown by the difference between the thick red lines and the black lines in Fig. 3. We already saw that the CMIP6 ensemble mean has a better agreement to the observed sea ice extent than does the CMIP5 ensemble mean (Fig. 1), and this is reflected in the annual-average extent in these two ensembles (Fig. 3). However, we can see from this

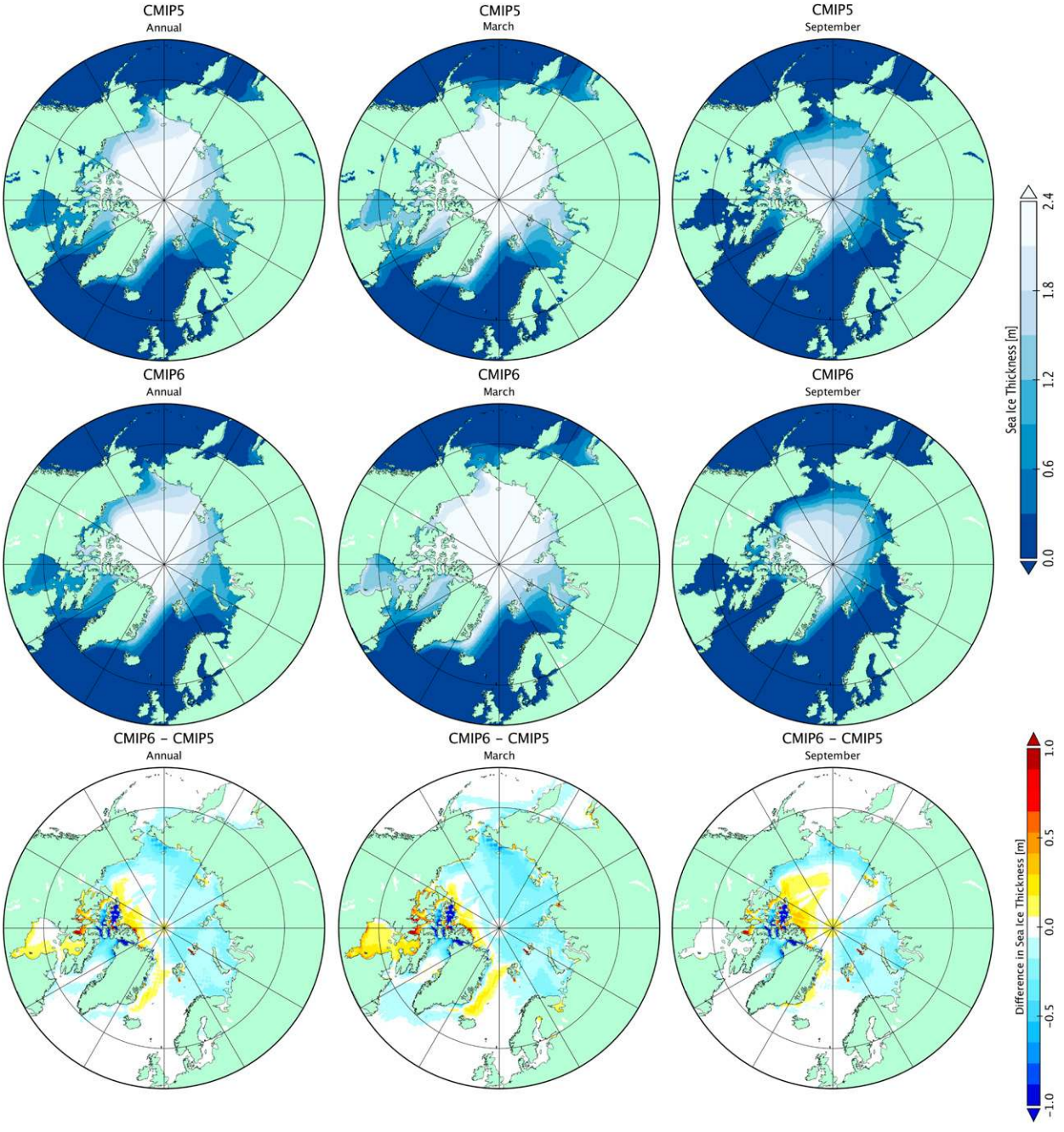

FIG. 2. The climatological mean sea ice thickness from the (top) CMIP5 and (middle) CMIP6 ensemble means, and (bottom) the difference between the two ensemble means, for (left) the annual mean and for the months of (center) March and (right) September, for the period 1979–2004.

persistent pattern of the models having thinner ice over the central Arctic and thicker ice in the Canadian archipelago that the improvements we saw in the overall Arctic sea ice volume in CMIP6 from Fig. 1 are due to compensating biases in the spatial distribution of sea ice, and that there is still a lot to be improved in the representation of sea ice thickness in these models. Much of the improvement in the sea ice extent in the CMIP6 ensemble comes from a better fit to the observed extent in the Barents Sea. We can see from the sea ice extent in March that this is due to an improved representation of the Barents Sea extent during the seasonal maximum. This is an important improvement in CMIP6 as coupled climate models have had long-standing biases toward

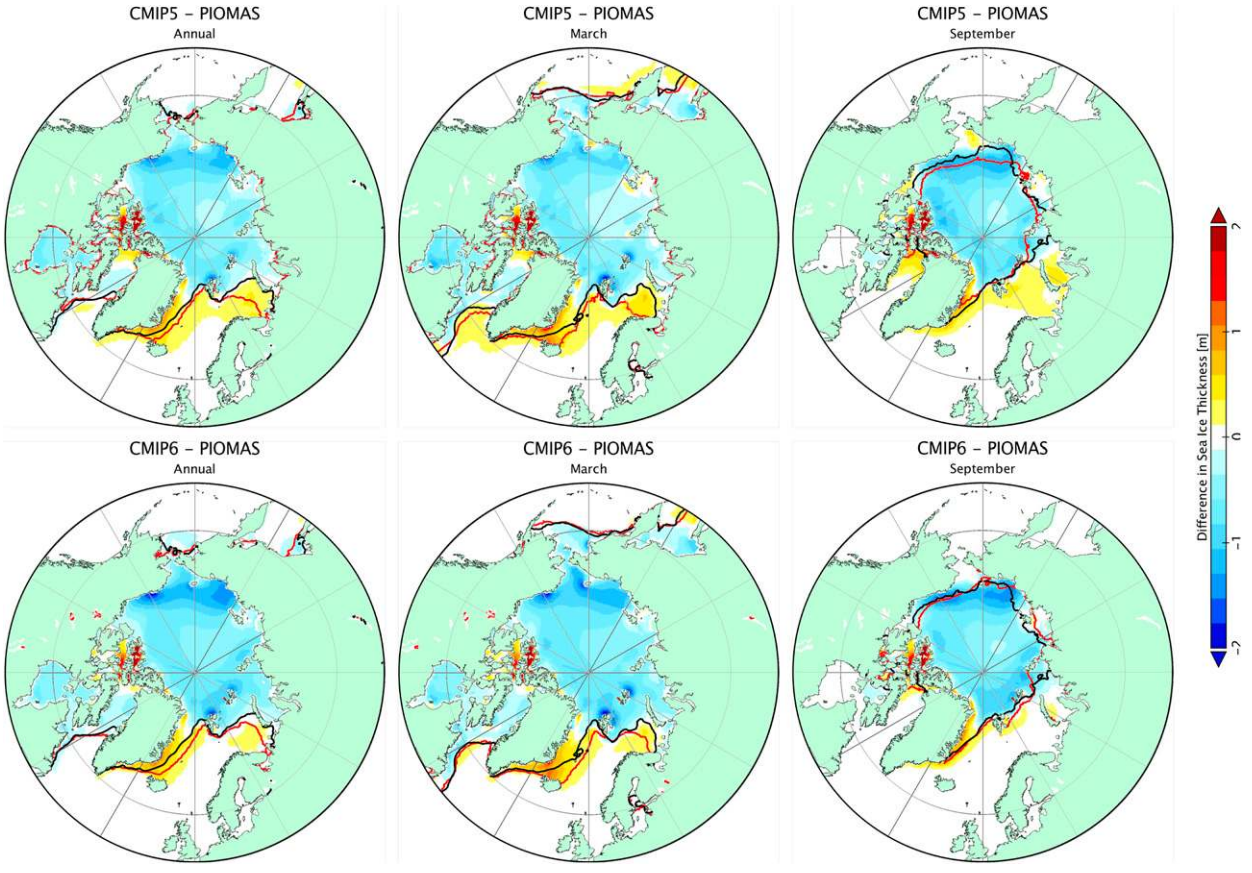

FIG. 3. The difference in the climatological mean sea ice thickness from the (top) CMIP5 and (bottom) CMIP6 ensemble means and the PIOMAS simulations for the months of (center) March and (right) September, and (left) for the annual mean for the period 1979–2004. The climatological mean sea ice extent from ERA5 is shown by the thick black line and from the ensemble means by the thick red line.

overestimating sea ice extent in this region (Ivanova et al. 2016). Despite this improvement, the CMIP6 models are still biased toward having too much sea ice in the Barents Sea in winter. In the CMIP5 ensemble the models tended to overestimate the sea ice extent in winter, which introduced large biases into the climate of the region and led to an intense focus on the processes of sea ice removal and formation in this region (Smedsrud et al. 2013).

There is generally a good fit to the observed sea ice extent in all other regions, except for a too high extent in Fram Strait, which is persistent in both the CMIP5 and CMIP6 ensembles. The climatologies in the seasonal maxima (March) and minima (September) in sea ice extent more clearly show the seasonality of this bias. In March both the CMIP5 and CMIP6 ensembles have a much too high extent in Fram Strait with sea ice extending to the coast of Iceland, which has not been seen in ERA5. This is likely linked to biases in the winter sea ice export through Fram Strait (Langehaug et al. 2013). In contrast, both the CMIP5 and CMIP6 ensembles have a good fit to the observed extent in Fram Strait in September, with the CMIP6 ensemble having an excellent fit to the observations at this time of year. However, another bias in September sea ice extent that has persisted between the CMIP5 and CMIP6 ensembles is that both have too little sea ice in the Kara Sea at the seasonal minima. This is a region where the September sea ice has been retreating during the period 1979–2004.

2) TRENDS AND VARIABILITY IN THE HISTORICAL PERIOD

This climatology is taken during a period of rapid decline in both the Arctic sea ice extent and volume. It is therefore necessary to also evaluate the ability of the current ensemble of climate models to capture the rate of decline in Arctic sea ice over this period. Figure 4 shows the trend in the sea ice extent and volume from the CMIP5 and CMIP6 ensembles compared to those from ERA5 and PIOMAS respectively. Almost all the CMIP model results for the historical period show a decline in the sea ice extent and volume during the

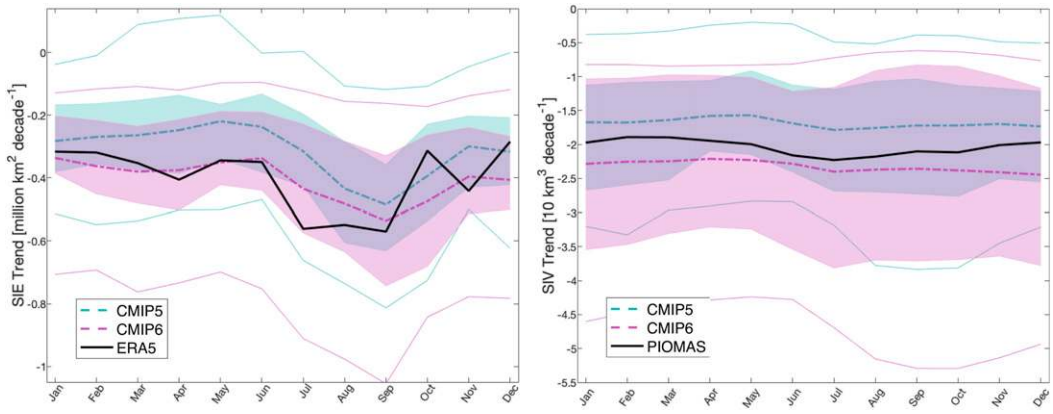

FIG. 4. The trend in the Arctic sea ice (left) extent and (right) volume for each month in the period 1979–2004. The CMIP5 models are shown in turquoise and the CMIP6 models in purple. The shaded areas show the range between the 25th and 75th percentiles of the model ensembles; the thick dashed lines show the ensemble mean; and the thin lines show the 5th and 95th percentiles of the ensemble. The thick black line shows the climatology from ERA5 for the extent and from PIOMAS for the volume.

period of our evaluation, 1979–2004. However, there is a very large spread in the trends between the different models. No individual model in either the CMIP5 or CMIP6 ensembles has a better fit (as measured by mean absolute difference) to the trends in sea ice extent from ERA5 than do the multimodel means. This may be expected given that individual models all have different tendencies due to natural variability in addition to the signal of declining sea ice due to enhanced radiative forcing.

In ERA5 there is a negative trend in the sea ice extent in all months, but there is also a pronounced seasonal cycle in the trend in sea ice extent with the most rapid decline in the summer months of July–September. The slowest decline occurs in December when the trend is $-25\,000\,\mathrm{km^2\,yr^{-1}}$ and the fastest decline occurs in September when the trend is $-55\,000\,\mathrm{km^2\,yr^{-1}}$, although this is very similar to the trends in July and August. This seasonal cycle is to some extent captured in the CMIP5 and CMIP6 multimodel means, which both have the peak decline in September. The CMIP6 ensemble mean has a better fit to the observed trends in September, and in the annual average, than does the CMIP5 ensemble mean. However, there is a very large spread in both the CMIP5 and CMIP6 ensembles with many models not having a clear seasonal cycle.

The trend in sea ice volume has a much lower seasonal cycle than the trend in extent, as might be expected. In PIOMAS the trend is very similar in all months with an average decrease of $-204\,\mathrm{km^3\,yr^{-1}}$. There is a weak seasonal cycle in PIOMAS with a minimum trend of $-189\,\mathrm{km^3\,yr^{-1}}$ in February and a peak trend of $-223\,\mathrm{km^3\,yr^{-1}}$ in July. Due to the small seasonal cycle, model biases in the trend in sea ice volume are principally systematic biases rather than seasonally dependent. Both the CMIP5 and CMIP6 models have a very large spread in the trends in sea ice volume, and so we cannot say there is any significant improvement in the representation of sea ice volume trends in CMIP6 over this period.

Another measure of the skill of the CMIP models in capturing the physics of sea ice, and sea ice driving forces, is to determine the degree of red noise in the system (i.e., how much the anomalies in one month are related to those in the previous month). Figure 5 shows the 1-month autoregressions in detrended anomalies of sea ice extent and volume for the CMIP5 and CMIP6 ensembles, in comparison to those found in ERA5 and PIOMAS for the extent and volume, respectively. We can see that in ERA5 the sea ice extent has a generally high autoregression, which ranges from $R = 0.24$ in June to $R = 0.82$ in September. There is a similar annual cycle to the autoregression in ERA5 as is found in the models with the highest predictability in September and lowest in June/July, but there is a higher autoregression found in the CMIP5 and CMIP6 models at all times of year. The model ensembles are very similar and both have two distinctive peaks in the seasonal cycle, one in March at the seasonal maxima in extent, and one in September at the seasonal minima in extent. The autoregression of extent anomalies is affected by many physical processes both dynamical and thermodynamical—for example, variability of oceanic heat transport from the Atlantic, atmospheric variability, and associated variations in atmospheric heat transport and wind-driven ice export. The causes of overly high autoregression in the models are therefore likely to be highly regional, but this requires further investigation.

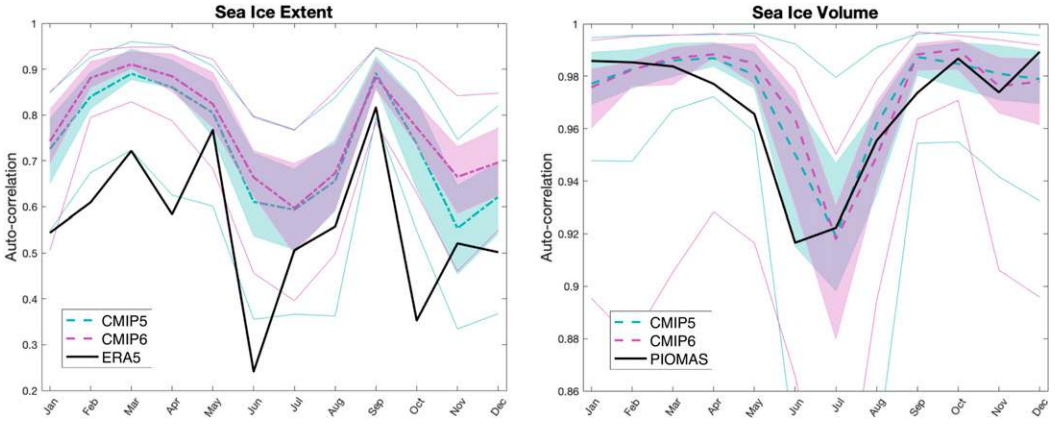

FIG. 5. The autoregression of the Arctic sea ice (left) extent and (right) volume for each month in the period 1979–2004. The CMIP5 models are shown in turquoise and the CMIP6 models in purple. The shaded areas show the range between the 25th and 75th percentiles of the model ensembles; the thick dashed lines show the ensemble mean; and the thin lines show the 5th and 95th percentiles of the ensemble. The thick black line shows the climatology from the ERA5 for the extent, and PIOMAS for the volume.

The autoregression of sea ice volume anomalies is even higher than that for extent. In the PIOMAS there is a clear seasonal cycle to the autoregression where it ranges from a minimum of $R = 0.92$ in June and July to a maximum of $R = 0.99$ in December. The autoregression in the reanalysis is generally lower than that found in the models but with a similar annual cycle. The CMIP5 and CMIP6 ensemble means are very similar and range from $R = 0.92$ in July to $R = 0.99$ in September. The slightly higher autoregression in the sea ice volume anomalies in the CMIP ensembles may be related to their bias toward too-deep ice in the Canadian archipelago, which is not as greatly affected by interannual variations in melting and ice transport as the rest of the sea ice pack.

There is a clear bias in both the CMIP5 and CMIP6 model ensembles to having a too-high persistency of anomalies in both sea ice extent and volume within the seasonal cycle. In the CMIP6 ensemble we might expect that this higher persistency is related to the overly thick ice in the Canadian archipelago as the ice in this region will not be readily melted or exported. The clearest example of that in the models is the predictability of September sea ice extent anomalies in the models based on the August extent: there is very little spread between the models, and they all have an extremely high predictability of the September sea ice extent. This could lead to overconfidence in the seasonal predictability of sea ice extent and volume from these models.

b. *Surface air temperature*

Figure 6 shows the climatology and the interannual variability of the Arctic-mean surface air temperature for each month from the CMIP5 and CMIP6 ensembles, and from ERA5, for the years 1979–2004. The climatological-mean seasonal cycle is almost identical in the CMIP5 and CMIP6 ensemble means. In the CMIP5 and CMIP6 ensemble means the temperature varies from a minimum of 245 K in January and February to a maximum of 275 K in July. There is a larger spread in the CMIP5 ensemble in the winter temperatures (December–February). The ensemble means of both CMIP5 and CMIP6 are colder than the reanalysis throughout the whole year, but the largest difference with ERA5 is in the winter: the ensemble means are more than 4° colder than the reanalysis in January and February. However, it is worth noting that comparisons with independent buoy observations in the Arctic have shown that ERA5 has a warm bias throughout the cold season, and this is especially strong in very cold conditions: the warm bias is around 2 K at 248 K (Wang et al. 2019).

This challenge with capturing the wintertime mean temperatures also extends to the interannual variability in winter temperatures. Throughout the wintertime both the CMIP5 and CMIP6 model ensemble means have a higher interannual variability than he ERA5. The biases in both the climatological mean and interannual variability of the surface air temperature are likely to be related as a colder surface climate is more sensitive to changes in forcing due to natural variability. One might expect these biases to also be related to the biases in the climatology of the sea ice detailed above; however, the models tend to have thinner sea ice but they are also colder than the reanalysis, contrary to expectation (Labe et al. 2018). This suggests that the sea ice and atmospheric components of the models have been independently tuned to reach a different default climatological balance between sea ice thickness and surface air temperature.

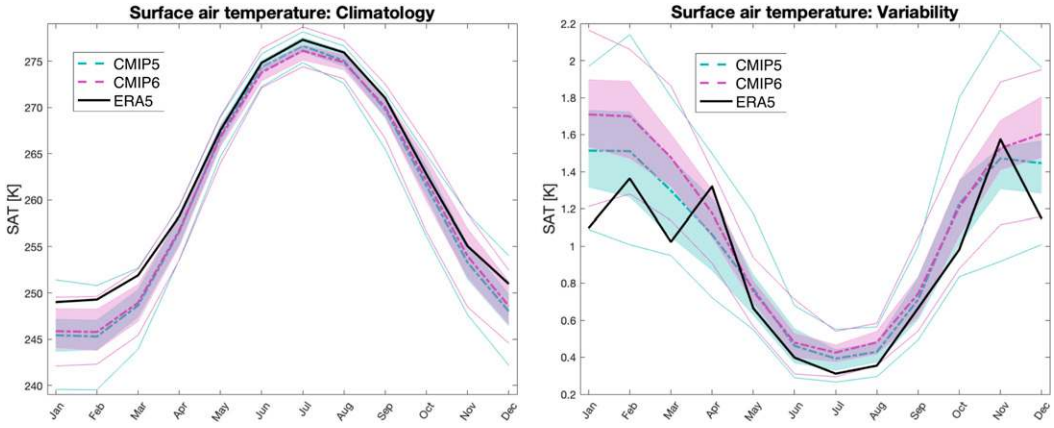

FIG. 6. The (left) climatological mean and (right) interannual variability of the surface air temperature averaged over the Arctic region for the years 1979 to 2004. The CMIP5 models are shown in turquoise and the CMIP6 models in purple. The shaded areas show the range between the 25th and 75th percentiles of the model ensembles; the thick dashed lines show the ensemble mean; and the thin lines show the 5th and 95th percentiles of the ensemble. The thick black line shows the result from ERA5.

Figure 7 shows the map of the climatological mean surface air temperature for the CMIP6 ensemble mean in the top row and the difference between the CMIP6 and CMIP5 ensemble means for the annual mean and for the months of January and July.

In the CMIP6 ensemble mean climatology the coldest region is over the interior of Greenland where the average surface air temperature is below the freezing point of water throughout the year. The largest differences between the CMIP6 and CMIP5 ensemble means are around the coast of Greenland and in the Barents Sea. In both of these regions the CMIP6 ensemble mean is warmer than the CMIP5 by around 2 K. The difference between these two ensembles is largest in the winter (January) in the Barents Sea, where temperature differences are around 4 K in the western Barents Sea. This is directly related to the reduced sea ice cover in this region in winter (Fig. 3) since without the insulating effect of sea ice, there are considerable energy fluxes from the ocean to the overlying atmosphere. This may affect the transport of warm moist air over land as we also see warmer temperatures over land in the whole Eastern Hemisphere. In the summer there is very little difference between the CMIP5 and CMIP6 ensemble means. There is almost zero difference over ice in the central Arctic where the air temperature is limited by the melting of sea ice, although the CMIP6 ensemble is much colder over the southern Canadian archipelago despite the generally thinner ice in these models in this region (Fig. 2). But even over land the temperature difference between the two ensembles is small, with the CMIP6 ensemble generally being approximately 1 K colder over land than the CMIP5 ensemble.

In comparison with ERA5, we can see that both the CMIP6 and CMIP5 ensembles are more than 1 K colder than the reanalysis over sea ice and the ocean in the annual mean (Fig. 8). Most of this bias is explained by differences in the wintertime temperatures as can be expected from Fig. 6. In both the CMIP5 and CMIP6 ensemble means we find cold biases of up to 9 K in regions with thick sea ice, such as off the coast of northern Greenland, but also in the regions where there is sea ice in the models but not in the reanalysis, such as in Fram Strait and in the Barents Sea (Fig. 8). The bias in the CMIP6 ensemble over thick sea ice is very similar to what was found in CMIP5, and most of the bias reduction in CMIP6 is associated with an improved representation of the sea ice edge in the Barents Sea and thereabouts.

In the summer (July) the pattern of bias is almost identical in the CMIP5 and CMIP6 ensembles. There is a general cool bias across most of the Arctic with an almost 1-K cold bias over ocean, sea ice, and almost all the land. The only clear exceptions are over the interior of Greenland where the model ensembles can have up to 5-K warm biases compared to the reanalysis. There are also strong warm biases over coastal waters everywhere in the Arctic, but especially in the Canadian archipelago. Note that one should be careful interpreting these, as there can be large differences around the coastlines due to the different land–sea masks used in the different CMIP models and the reanalysis.

One anticipated consequence of the thinning of sea ice is a reduction of the day-to-day variability in surface air temperature, since surface air temperatures over thick ice are more sensitive to forcing than the air over thin ice or open ocean (Esau et al. 2012) so the reduction

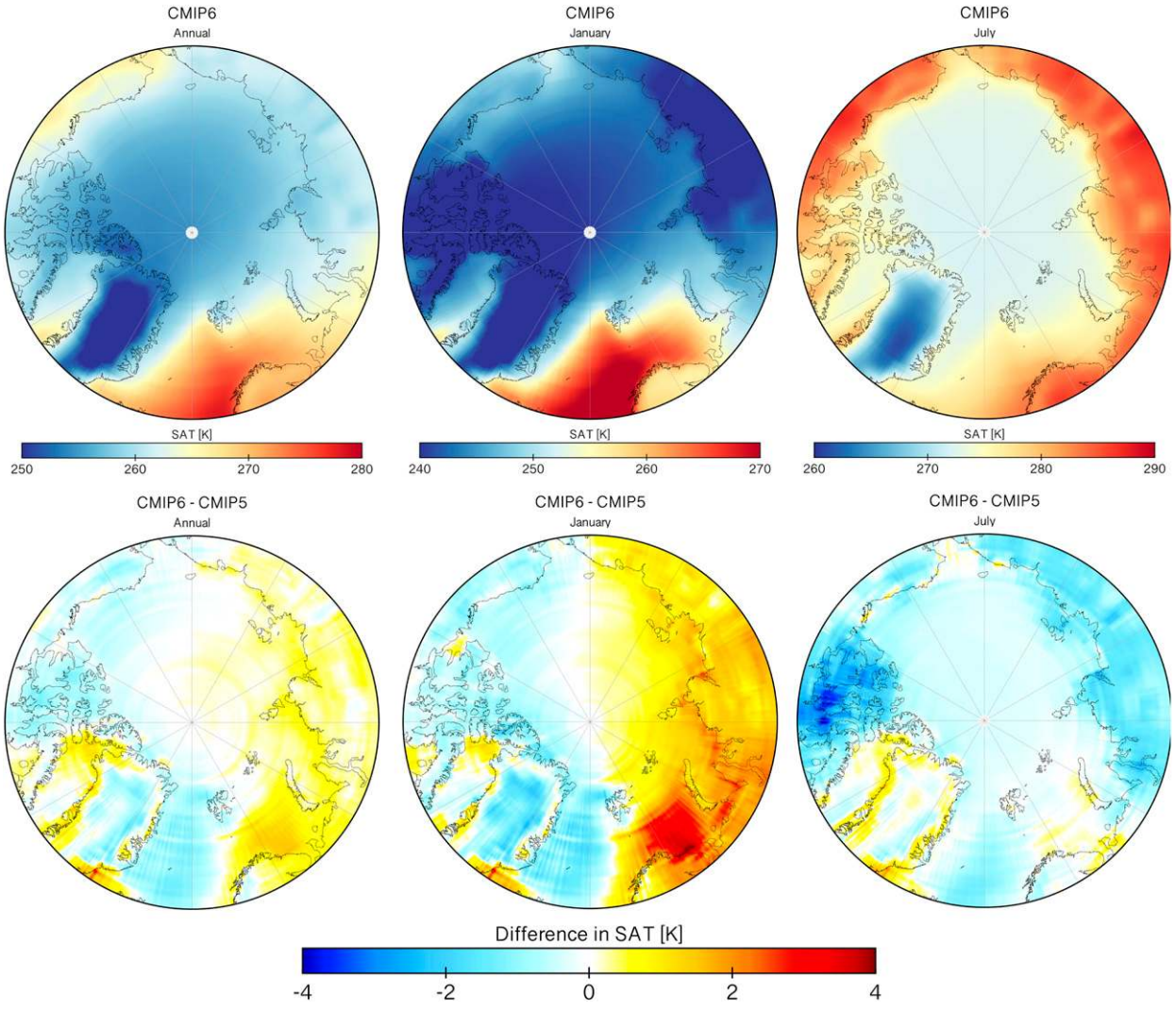

FIG. 7. (top) The climatological mean surface air temperature from the CMIP6 ensemble mean and (bottom) the difference between the climatologies in the CMIP6 and CMIP5 ensemble means for (left) the annual mean and the months of (center) January and (right) July. The top panels are plotted on different scales to ensure the spatial details are visible.

in sea ice cover should also result in a reduction in the SAT day-to-day variability. Another potential explanation for this is that as the surface warms the depth of the atmospheric mixed layer increases, which reduces the sensitivity of the surface air temperature to changes in forcing (Davy and Esau 2016). We can differentiate between these two explanations by evaluating where the reduction in variability is occurring geographically and by relating the changes in variability to the changes in sea ice extent at the seasonal extrema. However, this signal from long-term changes in climate forcing may be masked by the large natural variability in the Arctic, especially if the forced signal is a relatively weak effect. Figure 9 shows the trend in the day-to-day variability of surface air temperature from CMIP5, CMIP6, and ERA5.

In the annual mean both the CMIP5 and CMIP6 ensemble means have similar trends: there is a negative trend almost everywhere in the Arctic, with the largest reduction in day-to-day variability over the Barents, Chukchi, Beaufort, and eastern Siberian Seas. This pattern is very consistent between the two model ensembles, but it is quite different from the pattern found in the reanalysis. In ERA5 there is a negative trend across much of the Arctic, but there is a strong positive trend in the area north of Greenland.

The difference in the patterns in the annual mean can be explained by looking at the trends at the seasonal extrema in sea ice extent in March and September. In March the model ensembles have a negative trend across most of the Arctic, aside from the CMIP5 ensemble, which has a positive trend centered over the Canadian archipelago. However, this

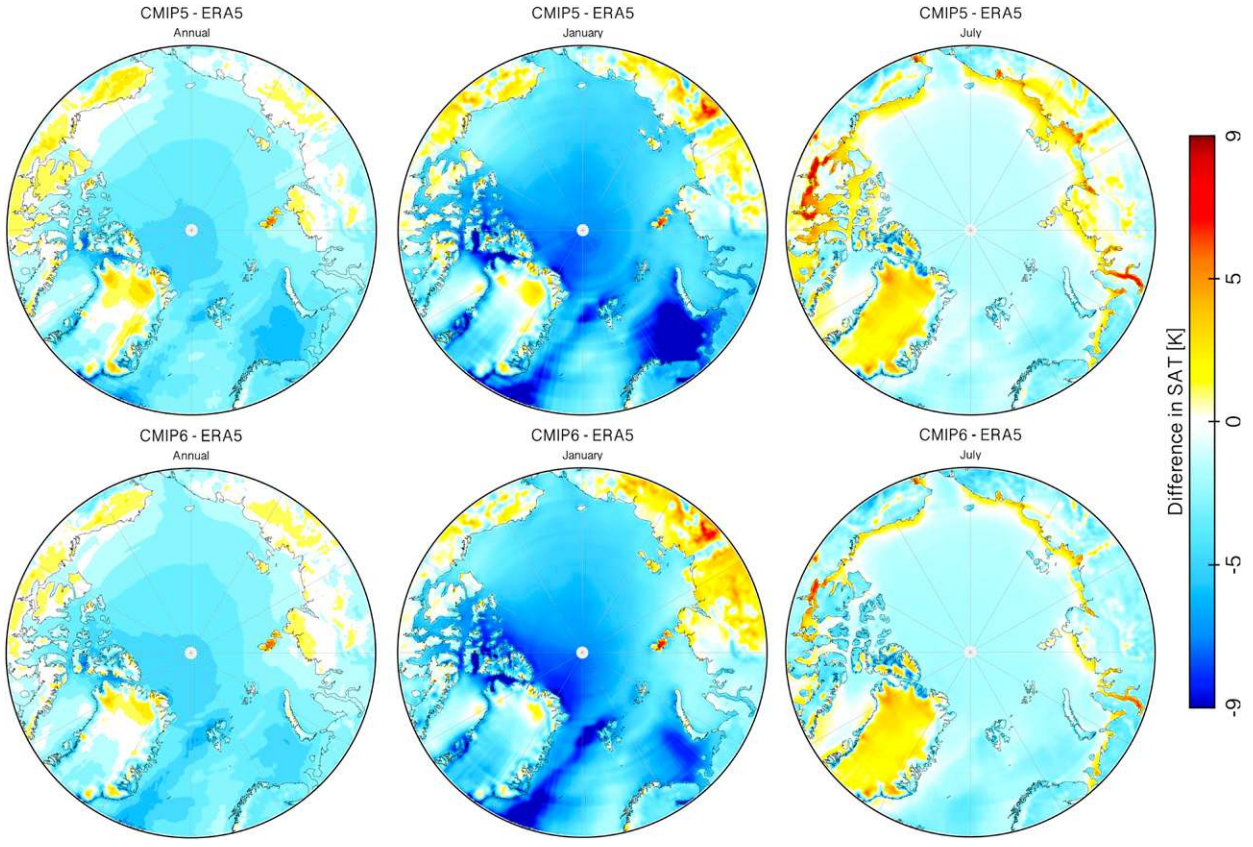

FIG. 8. The difference in the climatological mean 2-m air temperature between ERA5 and the multimodel means of (top) CMIP5 and (bottom) CMIP6 (left) in the annual mean and for the months of (center) January and (right) July over the period 1979–2004.

pattern is very different from what we find in ERA5 in March: at this time the reanalysis has a strong positive trend in the day-to-day variability across almost all the sea ice, and it is particularly strong in the area north of Greenland. This is the primary cause of the difference in the pattern of trends in the annual mean. During the seasonal minima in sea ice extent in September the model ensembles have better agreement with the reanalysis with a negative trend across all the sea ice, although in ERA5 there are very different patterns over land.

This large discrepancy between the CMIP simulations and ERA5 in the day-to-day variability may have a number of causes, including natural variability dominating over the forced signal in the reanalysis, biases in the synoptic activity (see next section), or limitations of the reanalysis. It may also be related to the biases in the climatology of the mean SAT (Fig. 8). The models tend to be too cold in winter across the entire Arctic Ocean, but especially in those regions with thick sea ice north of Greenland. Since colder conditions are more sensitive to changes in thermal or radiative forcing, this might explain why the models are biased toward too high day-to-day variability in SAT, and consequentially do not have the same response to forcing. Another likely cause is the limitations of the sea ice physics and surface coupling in these climate models. Many processes such as the dynamics of sea ice or the exchanges over leads in the ice are either poorly captured or altogether missing in climate models. However, these may play an important role in determining the low-level stability and surface fluxes, thus affecting the day-to-day variability. But since the reduction in variability is not limited to those regions where sea ice has been retreating over the period 1979–2004, it is likely that this reduction in variability is not solely due to changes in sea ice extent.

c. *Sea level pressure*

Here we use the monthly mean and the intramonthly variability in sea level pressure as measures of the atmospheric dynamics. The climatology and interannual variability of the monthly mean and the intramonthly variability in sea level pressure from the CMIP5 and CMIP6 ensembles and ERA5are shown in Fig. 10. The sea level pressure has a similar annual cycle in ERA5 as in the ensemble means with a peak in April–May followed by a sharp decline until July, although there is a large spread in both the CMIP5 and CMIP6 ensembles. However, the interannual variability of

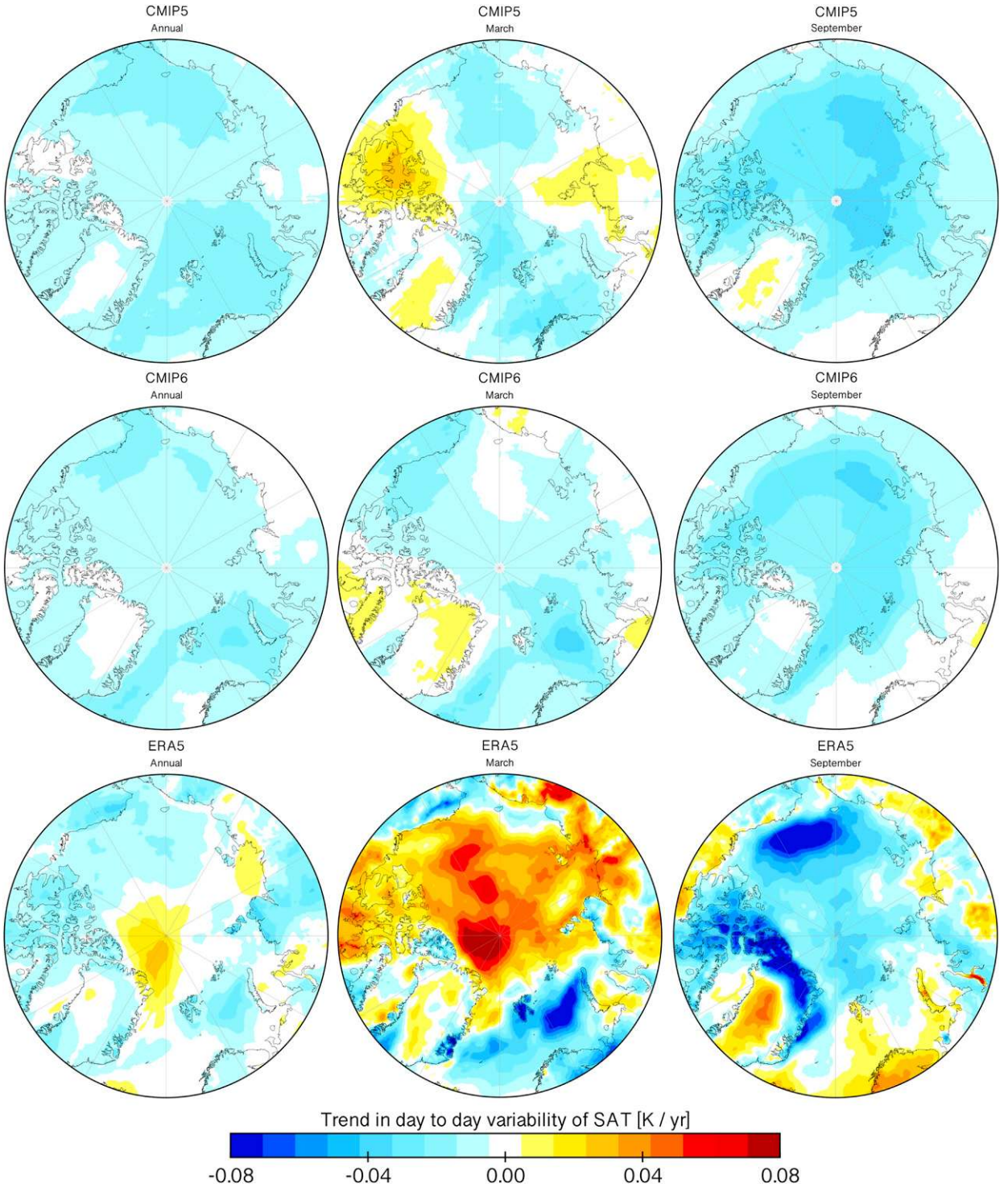

FIG. 9. The trend in the day-to-day variability in surface air temperature from the multimodel means of (top) CMIP5, (middle) CMIP6, and (bottom) ERA5 for (left) the annual mean, (middle) March, and (right) September over the period 1979–2004.

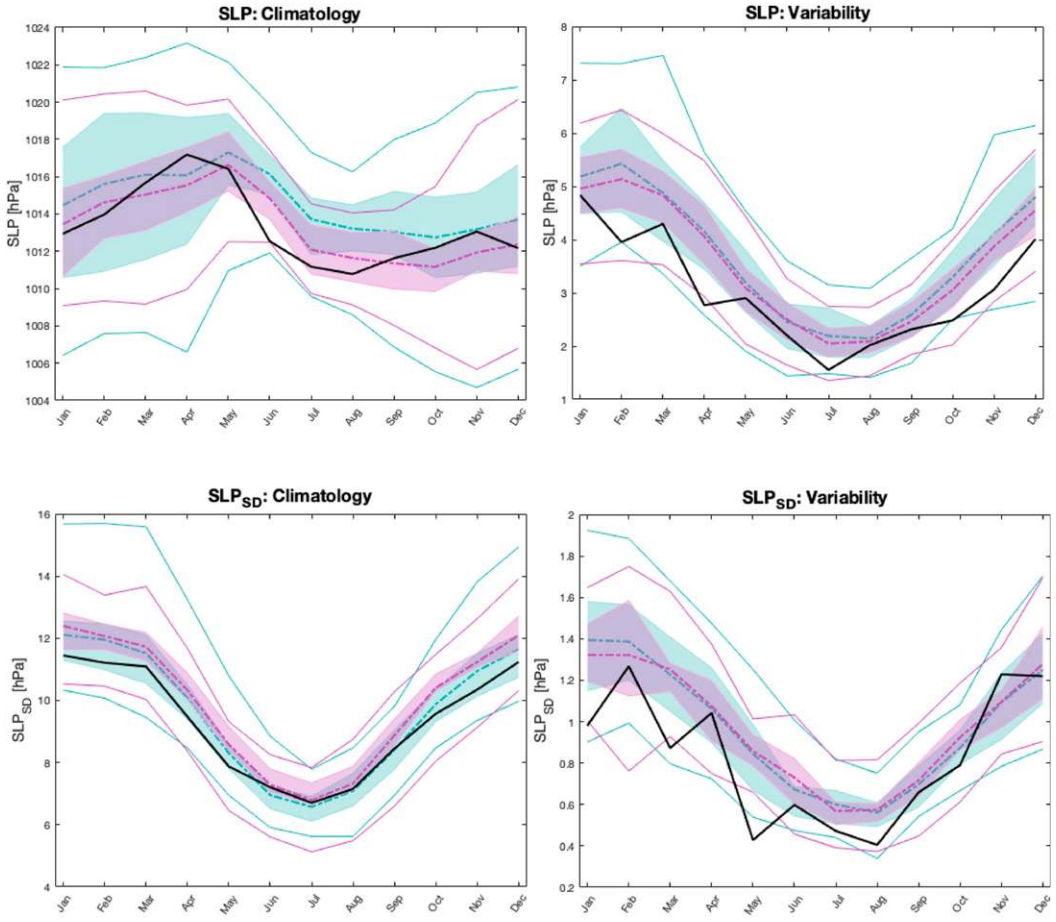

FIG. 10. The (top left) climatology and (top right) interannual variability of the monthly mean sea level pressure (SLP) and the (bottom left) climatology and (bottom right) interannual variability of the intramonthly standard deviation of the 6-hourly sea level pressure (SLP_{SD}) averaged over the Arctic region for the years 1979–2004. The CMIP5 models are shown in turquoise and the CMIP6 models in purple. The shaded areas show the range between the 25th and 75th percentiles of the model ensembles; the thick dashed lines show the ensemble mean; and the thin lines show the 5th and 95th percentiles of the ensemble. The thick black lines show the results from ERA5.

the monthly-mean sea level pressure is generally significantly higher in both CMIP5 and CMIP6 than in ERA5, although the annual cycle is very similar with a peak in January and minimum in July.

In ERA5 the intramonthly standard deviation of 6-hourly sea level pressure reaches a peak of around 5 hPa in the winter months (January–March), to a minimum of around 2.2 hPa in July. Overall, this is comparable to the multimodel means from CMIP5 and CMIP6. However, we can see from the CMIP5 and CMIP6 multimodel means that the climate models tend to overestimate the intramonthly variability, especially in the winter months. This tendency to overestimate the amount of synoptic activity in the Arctic winter months may be related to the model biases in day-to-day variability, although there is no significant correlation between model biases in the SLP variability and the SAT variability in either the CMIP5 or CMIP6 ensembles.

The models also show too-high variability in the interannual variability of synoptic activity, especially in the winter months (Fig. 10). However, the sudden drop in interannual variability in the January data in ERA5 is anomalous compared to the rest of the seasonal cycle, from which we might expect a peak in this month. The CMIP5 and CMIP6 multimodel means are very similar in the interannual variability and have variability similar to or greater than that found in ERA5 in the same period.

4. Projections for future change

The pace of climate change is currently fastest in the Arctic due to the various positive feedbacks found in this region (Serreze et al. 2007; Screen and Simmonds 2010; Pithan and Mauritsen 2014), and this is expected to continue throughout the twenty-first century, according to the IPCC

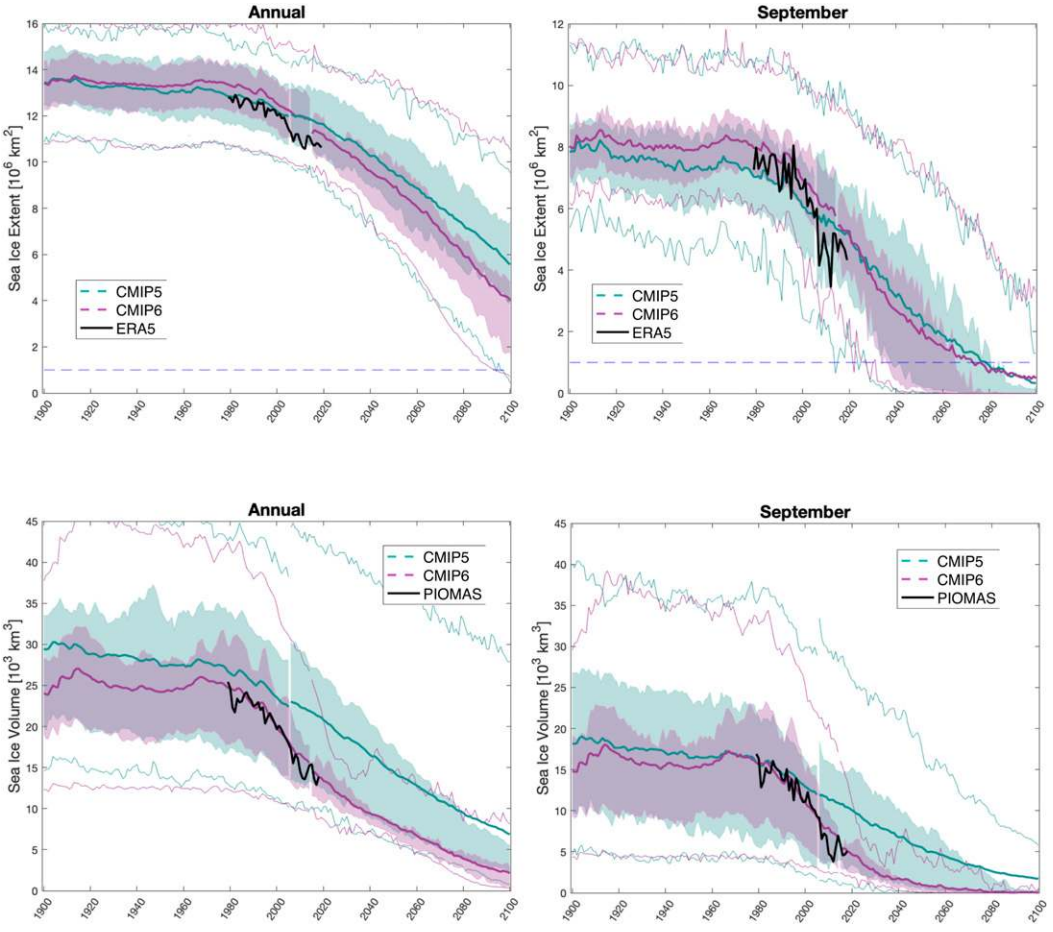

FIG. 11. Time series of sea ice (top) extent and (bottom) volume for (left) the annual mean and (right) the annual minima in September for the individual models and the ensemble mean from CMIP5 and CMIP6 compared with ERA5 for the extent and PIOMAS for the volume. The CMIP5 and CMIP6 models are shown in turquoise and purple, respectively, and the multimodel mean is highlighted by the thick line. The shaded areas show the range between the 25th and 75th percentiles of the model ensembles and the thin lines show the 5th and 95th percentiles of the ensemble. For the future period, CMIP5 and CMIP6 are shown for the RCP8.5 and SSP585 scenarios, respectively. The blue dashed line on the sea ice extent plot marks the limit of 1 million km^2, below which the Arctic is considered to be essentially ice-free.

Fifth Assessment Report (AR5). Even limiting the mean warming of Earth to 1.5 K will still mean a warming of around 3 K in the Arctic combined with a large loss of sea ice (Niederdrenk and Notz 2018). An important question under future forcing scenarios is how fast the Arctic sea ice will be removed and how confident we can be in those projections. The confidence can be assessed using the spread in the model ensemble running a given experiment, so it is highly relevant to assess model spread under the different CMIP6 forcing scenarios for the twenty-first century, and how this picture has changed since CMIP5.

a. Sea ice extent and volume

Figure 11 shows the time series of sea ice extent and volume from the CMIP5 and CMIP6 ensembles with comparison to ERA5 for the sea ice extent and to PIOMAS for the sea ice volume over the period 1900–2100. The CMIP5 ensemble uses the RCP8.5 forcing scenario for the years after 2005, and the CMIP6 results use the SSP585 scenario after the year 2014. Several of the SSP forcing scenarios were selected to provide continuity with the RCP scenarios used in CMIP5 including SSP585, which also reaches an increase in radiative forcing of 8.5 W m^{-2}, but following a pathway determined by integrated assessment models. See O'Neill et al. (2016) for a detailed comparison of the RCP and SSP scenarios. There is an almost identical sea ice extent in both the annual mean and the September minima in the CMIP5 and CMIP6 ensemble means prior to the 1990s. However, there is a very large spread in both the CMIP5 and CMIP6 ensembles during this period with almost all models having annual mean extents in the range of

11–16 million km^2, while the September minima have an even larger spread in this period with almost all models in the range of 5–12 million km^2. There is a very good fit between both the CMIP5 and CMIP6 ensemble means and the observed sea ice extent in the annual mean and September.

After the 1990s the sea ice extent was observed to rapidly reduce for the next 20 years, especially in the seasonal minima in September (Fig. 11). There was a slower reduction of sea ice extent in the CMIP5 ensemble than was observed since the mid-1990s. There has been a lot of speculation about the reasons for this (Stroeve et al. 2012), and it is likely that natural climate variability can help explain the discrepancy between the modeled and observed sea ice change (Swart et al. 2015). It could be because in the CMIP5 protocol in the post-2005 period only the CO_2 forcing was changing in time, whereas other forcings might have been important that were included in the CMIP6 historical protocol up until the year 2014. It is also likely that there are essential processes of sea ice coupling that are not included in these models that were important in causing this rapid decline. In the CMIP6 protocol the historical forcings extend up until 2014, and so cover part of this period of rapid decline (Eyring et al. 2016). There have also been efforts to address the depiction of sea ice in these models since CMIP5 (Kattsov et al. 2010). Some combination of these changes has led to an improvement in the CMIP6 ensemble mean over that from CMIP5. There is now a better fit to both the sea ice extent and volume found in reanalysis. However, there remain some important discrepancies between the CMIP6 models and the reanalysis.

This pattern of a more negative trend in CMIP6 than in CMIP5 continues into the twenty-first-century projections in comparison of the scenarios RCP8.5 and SSP585. These two twenty-first-century scenarios are not directly comparable, but they both correspond to the upper range of possible rates of change for the twenty-first century in the CMIP5 and CMIP6 protocols, respectively. In both the RCP8.5 and SSP585 scenarios we see a rapid decline in the sea ice extent, especially in September. Under the SSP585 scenario the multimodel mean reaches essentially ice-free conditions in September (less than 1 million km^2) by around 2060, whereas in the RCP8.5 this is not expected to be reached until around 2080. The difference between the RCP8.5 and SSP585 scenarios is also large in the projections for the annual mean extent: in the multimodel mean of the SSP585 projections the Arctic only has around 4 million km^2 by the end of the twenty-first century, whereas under RCP8.5 the CMIP5 models projected there to still be an annual average of around 6 million km^2 of sea ice.

While there is some indication of improvement in CMIP6 in the representation of historical sea ice extent, there is a clear improvement in the multimodel mean of sea ice volume. In the period from 1900 to the 1980s when the effect of CO_2 forcing was relatively weak, we can see there is still a very large spread in the CMIP6 ensemble projections of sea ice volume, comparable to that found in CMIP5. The CMIP5 and CMIP6 multimodel means are also very similar during this period. However, in the period from 1980 to present there was a very rapid decline in the sea ice volume, according to the PIOMAS reanalysis. While the CMIP5 ensemble mean underestimates the rate of decline of sea ice volume, this is extremely well captured by the multimodel mean of the CMIP6 models, both in the annual mean and the September minima (Fig. 11).

For the twenty-first-century projections the annual-mean sea ice volume is projected to have a near-linear decrease in time under the SSP585 scenario, getting very close to zero to the end of the twenty-first century. This contrasts with the RCP8.5 projections where the models begin the simulations with a higher overall volume and decrease over the twenty-first century at a similar rate to that found in the SSP585 projections, thus ending the twenty-first century with a volume of around 7000 km^3 compared to just 1000 km^3 in the CMIP6 ensemble.

A big difference with the CMIP6 protocol compared to that from CMIP5 was the construction of projections for the twenty-first century (O'Neill et al. 2016). In CMIP6 these scenarios are the result of integrated assessment models, which aim to provide more realistic future emissions scenarios. In Fig. 12 we compare projections from two of these scenarios, SSP126 and SSP585. These scenarios differ in how they assume that economic growth is fueled. In SSP126 the models assume that there is a relatively rapid uptake of non-fossil-fuel-based energy sources and other sustainability measures, whereas in SSP585 the models assume that economic growth continues to be largely enabled by the use of fossil fuels. Consequently, SSP585 is a high-emissions scenario and SSP126 is relatively low-emissions scenario. Figure 12 shows the projected sea ice extent and volume from CMIP6 models under these two scenarios.

There are substantial differences between the sea ice extent and cover under the different scenarios. Under SSP585 the Arctic is projected to be nearly ice-free in September by the mid-2050s, whereas under SSP126 this is not projected to happen. Under the SSP126 scenario the sea ice extent is projected to stabilize at around 9 million km^2 in the annual mean and 2.5 million km^2 in September by around 2060. This is in stark contrast to the SSP585 scenario where the extent continues to decline for the whole period.

There is a similar pattern with the sea ice volume. In the SSP126 scenario the volume continues to decline

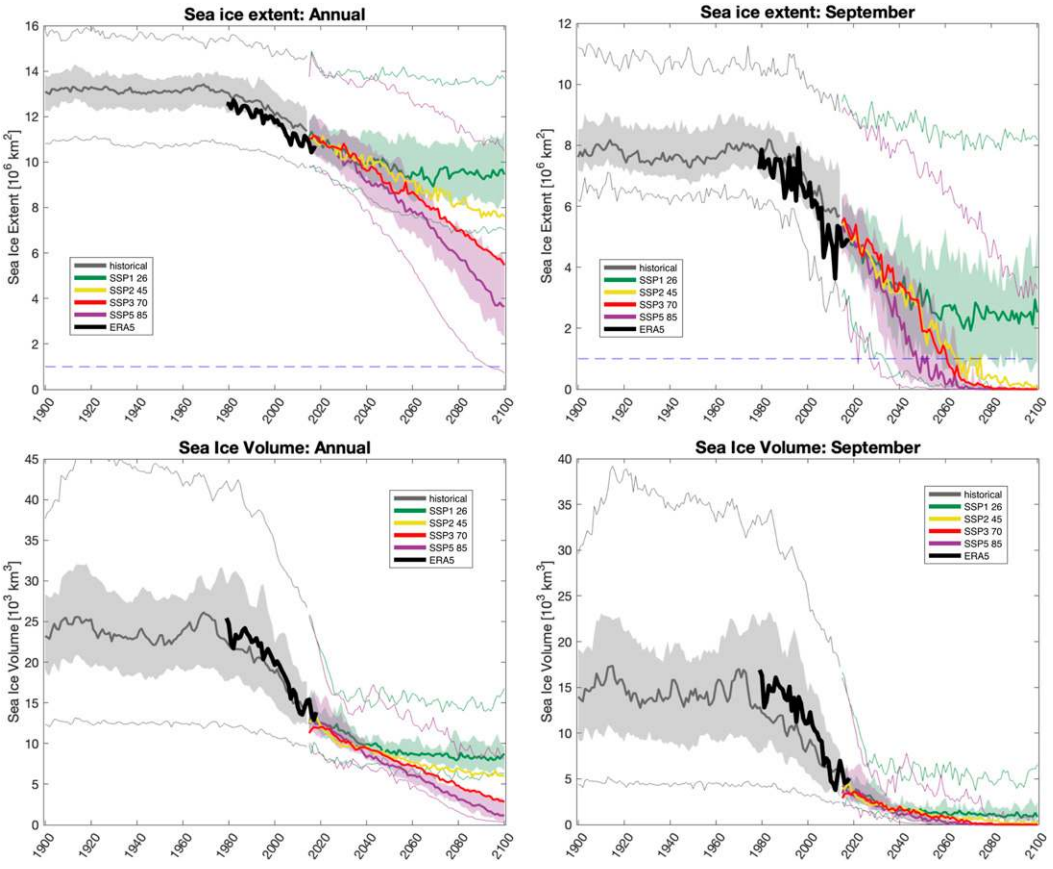

FIG. 12. Time series of sea ice (top) extent and (bottom) volume for (left) the annual mean and (right) the annual minima in September for the CMIP6 ensemble from the historical (gray), SSP126 (green), SSP245 (yellow), SSP370 (red), and SSP585 (purple) scenarios of CMIP6 compared with ERA5 for the extent and PIOMAS for the volume (black). The shaded areas show the range between the 25th and 75th percentiles of the model ensembles and the thin lines show the 5th and 95th percentiles of the ensemble. The multimodel means are highlighted by the thick lines.

until the mid-twenty-first century at which point it stabilizes at around 8000 km^3 in the annual mean and there is no significant trend in the volume for the second half of the twenty-first century. In contrast, in the SSP585 scenario the volume continues to decline for the whole of the twenty-first century. However, while the sea ice appears to stabilize by the mid-twenty-first century under SSP126, in this new climatological equilibrium the annual mean sea ice extent is around one-third less than what it was in the twentieth-century equilibrium. This difference is more pronounced with the sea ice volume, which stabilizes at an equilibrium where the annual mean is two-thirds lower than that of the twentieth century.

b. *Surface air temperature*

This rapid loss of sea ice is both caused by and contributes to a rapid increase in surface air temperatures in the Arctic, a phenomenon known as Arctic amplification (Serreze et al. 2007; Screen and Simmonds 2010). Previous analysis of CMIP5 models has shown that local thermal feedbacks are the dominant driver of Arctic amplification, but that the loss of sea ice also makes an important contribution to this phenomenon (Pithan and Mauritsen 2014).

Figure 13 shows the Arctic surface air temperature over the period of 1900–2100 contrasting the RCP8.5 scenario from CMIP5 and the SSP585 scenario from CMIP6. There is a clear, significant difference between the two scenarios for the twenty-first century. The multimodel means of the CMIP5 and CMIP6 historical temperatures up until 2005 are almost identical. The multimodel means of both scenarios increase almost linearly throughout the twenty-first century, but a slightly faster rate of warming under SSP585 leads to an Arctic approximately 5 K warmer in 2100 than is found under

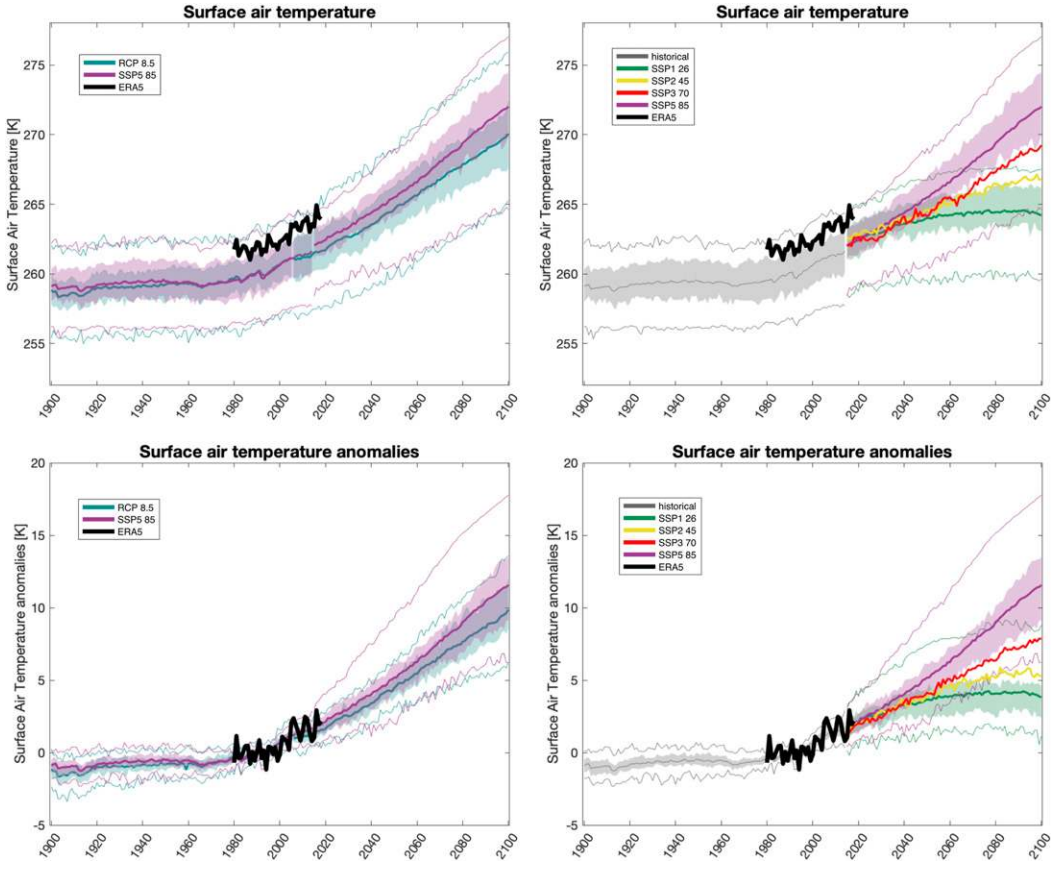

FIG. 13. Time series of the (top) absolute and (bottom) anomalies of surface air temperature over the period 1900–2100 (left) for CMIP5 combining the historical and RCP8.5 scenarios and CMIP6 combining the historical and SSP585 scenarios and (right) for CMIP6 comparing the projections for SSP126 and SSP585. The shaded areas show the range between the 25th and 75th percentiles of the model ensembles; the thick lines indicate the ensemble mean; and the thin lines show the 5th and 95th percentiles of the ensemble. Anomalies are taken with reference to the period 1980–2000.

RCP8.5, although the CMIP6 ensemble starts with a slightly warmer climate in 2015. Note that despite the significant difference between the two results there are outliers in both model ensembles such that there is a CMIP5 model that is warmer than the CMIP6 multimodel mean and a CMIP6 model that is colder than the CMIP5 multimodel mean throughout the twenty-first century.

Figure 13 also contrasts the SSP126 and SSP585 scenarios of CMIP6. We can clearly see that the two scenarios are virtually identical up until around 2040. This is due to the time it takes to implement decarbonization measures and the inertia of the climate system itself. Under SSP126 we can see the Arctic temperatures stabilizing by the mid-twenty-first century, as we saw for the sea ice (Fig. 13). This new, stable Arctic climate is on average 4.7 K warmer than was found in the previous equilibrium of the early twentieth century. This is almost 3 times the global average change in surface climate of 1.7 K under the SSP126 scenario. The corresponding changes in the temperature anomalies for the Arctic (the globe) in the other scenarios were 6.4 (2.5) K for SSP245, 7.9 (3.2) K for SSP370, 10.4 (4.3) K for SSP585, and 8.1 (3.4) K for RCP8.5. Therefore, we have a clear pattern of larger Arctic amplification—taken as the ratio of the two anomalies—under lower emission scenarios. It is worth noting that in a recent extreme-warm year (2016) we saw annual mean temperatures of similar magnitude to the projected twenty-first-century equilibrium under SSP126. This is due to the extremely high interannual variability found in the Arctic.

5. Summary

There have clearly been some improvements in CMIP6 compared to CMIP5 in capturing the state of the Arctic in

the recent decades. Some key points from the intercomparison of CMIP5 and CMIP6 skill are the following:

- There is better representation of the sea ice extent, edge, and retreat in CMIP6, in particular in the Barents Sea. This was an important bias in the Arctic climate in the CMIP5 simulations, and the CMIP6 models have a much smaller bias in the mean extent, and a closer fit to the observed decline in sea ice extent in this region. This is a key location for atmosphere–ocean coupling and an improved representation of the sea ice extent here could have consequences for midlatitude climate (Outten et al. 2013) and the representation of multidecadal variability (Outten et al. 2018).
- The climatology of the sea ice volume in CMIP6 shows a better fit to PIOMAS than did CMIP5. The CMIP6 ensemble mean is an extremely good fit to the observed decline in sea ice volume over the period 1979–2018. However, there remains a large spread within the CMIP6 ensemble as to the climatology of the sea ice volume in the twentieth century. And, as we found in CMIP5, there are large compensating biases of too-thick sea ice around the Canadian archipelago and too-thin ice elsewhere, compared to PIOMAS.
- Both CMIP5 and CMIP6 models generally have too-high persistency of anomalies in the sea ice extent compared to observations. This means that these models all tend to overestimate the predictability of sea ice extent.
- Both the CMIP5 and CMIP6 models have on average a 4-K cold bias over the Arctic in winter (January and February). This cold bias covers most of the Arctic but is particularly strong in the regions where the models overestimate the ice cover (the Barents Sea and the Fram Strait) and where the ice is thick (north of Greenland) or poorly resolved due to the presence of many islands not resolved in the climate models (Canadian archipelago).
- The CMIP5 and CMIP6 models tend to overestimate the interannual variability in wintertime temperatures in the Arctic. This bias is larger in the CMIP6 ensemble than in the CMIP5 ensemble.
- Both the CMIP5 and CMIP6 models show a reduction in the day-to-day variability of surface air temperature over the period 1979–2004. But this is not consistent with ERA5, which shows an increase in day-to-day variability over sea ice in winter during this period. This could be due to natural variability, missing or poorly represented surface coupling processes in the climate models that are important in the winter, or an inaccuracy of the reanalysis.
- In the high-emission scenario of CMIP6, SSP585, the Arctic is projected to be nearly ice-free in September by the mid-twenty-first century. However, in the low-emission SSP126 scenario of CMIP6 the sea ice extent is projected to stabilize by around 2040 at approximately 2.5 million km^2. So, if the global economy rapidly decarbonizes following the SSP126 pathway there is a better than 50% chance that there will not be ice-free Septembers in the Arctic.
- Under the SSP126 scenario of CMIP6 the Arctic air temperatures will also stabilize by around 2040 at 4.7 K warmer than the 1950–80 average, which is almost 3 times the global average warming for this period of 1.7 K.
- All scenarios in CMIP6 exhibit a strong Arctic amplification with Arctic anomalies at the end of the twenty-first century (2070–2100) at least 2.4 times larger than the respective global temperature anomalies.

Acknowledgments. This publication was support by the Norwegian Research Council projects INES and KeyCLIM, and the Bjerknes Center for Climate Research's Fast Track Initiative program. The PIOMAS reanalysis data of sea ice thickness are made available by the University of Washington (http://psc.apl.uw.edu/data/). The CMIP5 and CMIP6 data are made available by the ESGF and the data can be acquired from the ESGF nodes (e.g., https://esgf-data.dkrz.de/projects/esgf-dkrz/). The ERA5 atmospheric reanalysis dataset is produced and provided by the European Centre for Medium-Range Weather Forecasts and can be acquired via their portal (https://apps.ecmwf.int/data-catalogues/era5/).

REFERENCES

Boé, J., A. Hall, and X. Qu, 2010: Sources of spread in simulations of Arctic sea ice loss over the twenty-first century. *Climatic Change*, **99**, 637–645, https://doi.org/10.1007/s10584-010-9809-6.

Brigham-Grette, J., and Coauthors, 2013: Pliocene warmth, polar amplification, and stepped Pleistocene cooling recorded in NE Arctic Russia. *Science*, **340**, 1421–1427, https://doi.org/10.1126/science.1233137.

Chapman, W. L., and J. E. Walsh, 2007: Simulations of Arctic temperature and pressure by global coupled models. *J. Climate*, **20**, 609–632, https://doi.org/10.1175/JCLI4026.1.

Dahl-Jensen, D., K. Mosegaard, N. Gundestrup, G. D. Clow, S. J. Johnsen, A. W. Hansen, and N. Balling, 1998: Past temperatures directly from the Greenland Ice Sheet. *Science*, **282**, 268–271, https://doi.org/10.1126/science.282.5387.268.

Dai, A., D. Luo, M. Song, and J. Liu, 2019: Arctic amplification is caused by sea ice loss under increasing CO_2. *Nat. Commun.*, **10**, 121, https://doi.org/10.1038/s41467-018-07954-9.

Davy, R., 2018: The climatology of the atmospheric boundary layer in contemporary global climate models. *J. Climate*, **31**, 9151–9173, https://doi.org/10.1175/JCLI-D-17-0498.1.

——, and I. Esau, 2014: Global climate models' bias in surface temperature trends and variability. *Environ. Res. Lett.*, **9**, 114024, https://doi.org/10.1088/1748-9326/9/11/114024.

——, and ——, 2016: Differences in the efficacy of climate forcings explained by variations in atmospheric boundary layer depth.

Nat. Commun., **7**, 11690, https://doi.org/10.1038/ncomms11690.

Descamps, S., and Coauthors, 2017: Climate change impacts on wildlife in a High Arctic archipelago—Svalbard, Norway. *Global Change Biol.*, **23**, 490–502, https://doi.org/10.1111/gcb.13381.

Esau, I., R. Davy, and S. Outten, 2012: Complementary explanation of temperature response in the lower atmosphere. *Environ. Res. Lett.*, **7**, 044026, https://doi.org/10.1088/1748-9326/7/4/044026.

Eyring, V., S. Bony, G. A. Meehl, C. A. Senior, B. Stevens, R. J. Stouffer, and K. E. Taylor, 2016: Overview of the Coupled Model Intercomparison Project Phase 6 (CMIP6) experimental design and organization. *Geosci. Model Dev.*, **9**, 1937–1958, https://doi.org/10.5194/gmd-9-1937-2016.

Frederiksen, L-E., 2018: An evaluation of the reanalysed ERA-Interim and ERA5 in the Arctic using N-ICE2015 data. Master's thesis, Dept. of Physics and Technology, University in Tromso, 79 pp., https://hdl.handle.net/10037/13509.

Graham, R. M., S. R. Hudson, and M. Maturilli, 2019: Improved performance of ERA5 in Arctic gateway relative to four global atmospheric reanalyses. *Geophys. Res. Lett.*, **46**, 6138–6147, https://doi.org/10.1029/2019GL082781.

Graversen, R. G., and M. Wang, 2009: Polar amplification in a coupled climate model with a locked albedo. *Climate Dyn.*, **33**, 629–643, https://doi.org/10.1007/s00382-009-0535-6.

Ivanova, D. P., P. J. Gleckler, K. E. Taylor, P. J. Durack, and K. D. Marvel, 2016: Moving beyond the total sea ice extent in gauging model biases. *J. Climate*, **29**, 8965–8987, https://doi.org/10.1175/JCLI-D-16-0026.1.

Johannessen, O. M., and Coauthors, 2004: Arctic climate change: Observed and modelled temperature and sea-ice variability. *Tellus*, **56A**, 328–341, https://doi.org/10.3402/tellusa.v56i4.14418.

Karlsson, J., and G. Svensson, 2013: Consequences of poor representation of Arctic sea ice albedo and cloud-radiation interactions in the CMIP5 model ensemble. *Geophys. Res. Lett.*, **40**, 4374–4379, https://doi.org/10.1002/grl.50768.

Kattsov, V. M., V. E. Ryabinin, J. E. Overland, M. C. Serreze, M. Visbeck, J. E. Walsh, W. Meier, and X. Zhang, 2010: Arctic sea ice change: A grand challenge of climate science. *J. Glaciol.*, **56**, 1115–1121, https://doi.org/10.3189/002214311796406176.

Koenigk, T., A. Devasthale, and K.-G. Karlsson, 2014: Summer Arctic sea ice albedo in CMIP5 models. *Atmos. Chem. Phys.*, **14**, 1987–1998, https://doi.org/10.5194/acp-14-1987-2014.

Kumar, A., and Coauthors, 2010: Contribution of sea ice loss to Arctic amplification. *Geophys. Res. Lett.*, **37**, L21701, https://doi.org/10.1029/2010GL045022.

Kwok, R., 2015: Sea ice convergence along the Arctic coasts of Greenland and the Canadian Arctic Archipelago: Variability and extremes (1992–2014). *Geophys. Res. Lett.*, **42**, 7598–7605, https://doi.org/10.1002/2015GL065462.

——, 2018: Arctic sea ice thickness, volume, and multiyear ice coverage: Losses and coupled variability (1958–2018). *Environ. Res. Lett.*, **13**, 105005, https://doi.org/10.1088/1748-9326/aae3ec.

——, G. F. Cunningham, M. Wensnaham, I. Rigor, H. J. Zwally, and D. Yi, 2009: Thinning and volume loss of the Arctic Ocean sea ice cover: 2003–2008. *J. Geophys. Res.*, **114**, C07005, https://doi.org/10.1029/2009JC005312.

Labe, Z., Y. Peings, and G. Magnusdottir, 2018: Contributions of ice thickness to the atmospheric response from projected Arctic sea ice loss. *Geophys. Res. Lett.*, **45**, 5635–5642, https://doi.org/10.1029/2018GL078158.

Langehaug, H. R., F. Geyer, L. H. Smedsrud, and Y. Gao, 2013: Arctic sea ice decline and ice export in the CMIP5 historical simulations. *Ocean Modell.*, **71**, 114–126, https://doi.org/10.1016/j.ocemod.2012.12.006.

Lesins, G., T. J. Duck, and J. R. Drummond, 2012: Surface energy balance framework for Arctic amplification of climate change. *J. Climate*, **25**, 8277–8288, https://doi.org/10.1175/JCLI-D-11-00711.1.

Manabe, S., and R. Wetherald, 1975: The effects of doubling the CO_2 concentration on the climate of a general circulation model. *J. Atmos. Sci.*, **32**, 3–15, https://doi.org/10.1175/1520-0469(1975)032<0003:TEODTC>2.0.CO;2.

Maslowski, W., J. Clement Kinney, M. Higgins, and A. Roberts, 2012: The future of Arctic sea ice. *Annu. Rev. Earth Planet. Sci.*, **40**, 625–654, https://doi.org/10.1146/annurev-earth-042711-105345.

Masson-Delmotte, V., and Coauthors, 2006: Past and future polar amplification of climate change: Climate model intercomparisons and ice-core constraints. *Climate Dyn.*, **26**, 513–529, https://doi.org/10.1007/s00382-005-0081-9.

Massonnet, F., T. Fichefet, H. Goosse, C. M. Bitz, G. Philippon-Berthier, M. M. Holland, and P.-Y. Barriat, 2012: Constraining projections of summer Arctic sea ice. *Cryosphere*, **6**, 1383–1394, https://doi.org/10.5194/tcd-6-2931-2012.

Melia, N., K. Haines, and E. Hawkins, 2016: Sea ice decline and 21st century trans-Arctic shipping routes. *Geophys. Res. Lett.*, **43**, 9720–9728, https://doi.org/10.1002/2016GL069315.

Mortin, J., R. G. Graversen, and G. Svensson, 2014: Evaluation of pan-Arctic melt-freeze onset in CMIP5 climate models and reanalyses using surface observation. *Climate Dyn.*, **42**, 2239–2257, https://doi.org/10.1007/s00382-013-1811-z.

Niederdrenk, A. L., and D. Notz, 2018: Arctic sea ice in a 1.5°C warmer world. *Geophys. Res. Lett.*, **45**, 1963–1971, https://doi.org/10.1002/2017GL076159.

Notz, D., and J. Stroeve, 2018: The trajectory towards a seasonally ice-free Arctic Ocean. *Curr. Climate Change Rep.*, **4**, 407–416, https://doi.org/10.1007/s40641-018-0113-2.

Outten, S., R. Davy, and I. Esau, 2013: Eurasian winter cooling: Intercomparison of reanalyses and CMIP5 data sets. *Atmos. Ocean. Sci. Lett.*, **6**, 324–331, https://doi.org/10.1080/16742834.2013.11447102.

——, I. Esau, and O. H. Otterå, 2018: Bjerknes compensation in the CMIP5 climate models. *J. Climate*, **31**, 8745–8760, https://doi.org/10.1175/JCLI-D-18-0058.1.

Overland, J. E., and M. Wang, 2010: Large-scale atmospheric circulation changes are associated with the recent loss of Arctic sea ice. *Tellus*, **62A**, 1–9, https://doi.org/10.1111/j.1600-0870.2009.00421.x.

——, and ——, 2013: When will the summer Arctic be nearly sea ice free? *Geophys. Res. Lett.*, **40**, 2097–2101, https://doi.org/10.1002/grl.50316.

O'Neill, B. C., and Coauthors, 2016: The Scenario Model Intercomparison Project (ScenarioMIP) for CMIP6. *Geosci. Model Dev.*, **9**, 3461–3482, https://doi.org/10.5194/gmd-9-3461-2016.

Pavlova, T. V., V. M. Kattsov, and V. F. Govorkova, 2011: Sea ice in CMIP5: Closer to reality? (in Russian). *Tr. GGO*, **564**, 7–18.

Pithan, F., and T. Mauritsen, 2014: Arctic amplification dominated by temperature feedbacks in contemporary climate models. *Nat. Geosci.*, **7**, 181–184, https://doi.org/10.1038/ngeo2071.

——, B. Medeiros, and T. Mauritsen, 2014: Mixed-phase clouds cause climate model biases in Arctic wintertime temperature inversions. *Climate Dyn.*, **43**, 289–303, https://doi.org/10.1007/s00382-013-1964-9.

Planck, M., 1901: Ueber das Gesetz der Energieverteilung im Normalspectrum. *Ann. Phys.*, **309**, 553–563, https://doi.org/10.1002/andp.19013090310.

Schweiger, A., R. Lindsay, J. Zhang, M. Steele, H. Stern, and R. Kwok, 2011: Uncertainty in modeled Arctic sea ice volume. *J. Geophys. Res.*, **116**, C00D06, https://doi.org/10.1029/2011JC007084.

Screen, J. A., 2018: Arctic sea ice at 1.5 and 2°C. *Nat. Climate Change*, **8**, 362–363, https://doi.org/10.1038/s41558-018-0137-6.

——, and I. Simmonds, 2010: The central role of diminishing sea ice in recent Arctic temperature amplification. *Nature*, **464**, 1334–1337, https://doi.org/10.1038/nature09051.

Seidel, D. J., Y. Zhang, A. Beljaars, J.-C. Golaz, A. R. Jacobson, and B. Medeiros, 2012: Climatology of the planetary boundary layer over the continental United States and Europe. *J. Geophys. Res.*, **117**, D17106, https://doi.org/10.1029/2012JD018143.

Serreze, M. C., M. M. Holland, and J. Stroeve, 2007: Perspectives on the Arctic's shrinking sea ice cover. *Science*, **315**, 1533–1536, https://doi.org/10.1126/science.1139426.

——, A. P. Barrett, J. C. Stroeve, D. N. Kindig, and M. M. Holland, 2009: The emergence of surface-based Arctic amplification. *Cryosphere*, **3**, 11–19, https://doi.org/10.5194/tc-3-11-2009.

Sigmond, M., J. C. Fyfe, and N. C. Swart, 2018: Ice-free Arctic projections under the Paris Agreement. *Nat. Climate Change*, **8**, 404–408, https://doi.org/10.1038/s41558-018-0124-y.

Smedsrud, L. H., and Coauthors, 2013: The role of the Barents Sea in the Arctic climate system. *Rev. Geophys.*, **51**, 415–449, https://doi.org/10.1002/rog.20017.

Smith, L. C., and S. R. Stephenson, 2013: New trans-Arctic shipping routes navigable by midcentury. *Proc. Natl. Acad. Sci. USA*, **110**, E1191–E1195, https://doi.org/10.1073/pnas.1214212110.

Spielhagen, R. F., and Coauthors, 2011: Enhanced modern heat transfer to the arctic by warm Atlantic water. *Science*, **331**, 450–453, https://doi.org/10.1126/science.1197397.

Steeneveld, G. J., 2014: Current challenges in understanding and forecasting stable boundary layers over land and ice. *Front. Environ. Sci.*, **2**, 41, https://doi.org/10.3389/fenvs.2014.00041.

Stroeve, J., V. Kattsov, A. Barrett, M. Serreze, T. Pavlova, M. Holland, and W. N. Meier, 2012: Trends in Arctic sea ice extent from CMIP5, CMIP3 and observations. *Geophys. Res. Lett.*, **39**, L16502, https://doi.org/10.1029/2012GL052676.

Swart, N. C., J. C. Fyfe, E. Hawkins, J. E. Kay, and A. Jahn, 2015: Influence of internal variability on Arctic sea ice trends. *Nat. Climate Change*, **5**, 86–89, https://doi.org/10.1038/nclimate2483.

Tan, I., T. Storelvmo, and M. D. Zelinka, 2016: Observational constraints on mixed-phase clouds imply higher climate sensitivity. *Science*, **352**, 224–227, https://doi.org/10.1126/science.aad5300.

Vavrus, S., 2004: The impact of cloud feedbacks on Arctic climate under greenhouse forcing. *J. Climate*, **17**, 603–615, https://doi.org/10.1175/1520-0442(2004)017<0603:TIOCFO>2.0.CO;2.

Wang, C., R. M. Graham, K. Wang, S. Gerland, and M. A. Granskog, 2019: Comparison of ERA5 and ERA-Interim near-surface air temperature, snowfall and precipitation over Arctic sea ice: Effects on sea ice thermodynamics and evolution. *Cryosphere*, **13**, 1661–1679, https://doi.org/10.5194/tc-13-1661-2019.

Wang, M., and J. E. Overland, 2012: A sea ice free summer Arctic within 30 years: An update from CMIP5 models. *Geophys. Res. Lett.*, **39**, L18501, https://doi.org/10.1029/2012GL052868.

Zhang, J., and D. A. Rothrock, 2003: Modeling global sea ice with a thickness and enthalpy distribution model in generalized curvilinear coordinates. *Mon. Wea. Rev.*, **131**, 845–861, https://doi.org/10.1175/1520-0493(2003)131<0845:MGSIWA>2.0.CO;2.

Zygmuntowska, M., P. Rampal, N. Ivanova, and L. H. Smedsrud, 2014: Uncertainties in Arctic sea ice thickness and volume: New estimates and implications for trends. *Cryosphere*, **8**, 705–720, https://doi.org/10.5194/tc-8-705-2014.